GEOLOGICAL SURVEY OF CANADA

OPEN FILE 7264

Methodology for Assessing Prospectivity for Gold Deposits in the Canadian Shield

C. Chung, J.M. Franklin, B. Dubé and E.M. Hillary

2012

Natural Resources Canada | Ressources naturelles Canada

Canada

GEOLOGICAL SURVEY OF CANADA
OPEN FILE 7264

Methodology for Assessing Prospectivity for Gold Deposits in the Canadian Shield

C. Chung, J.M. Franklin, B. Dubé, and E.M. Hillary

2012

doi:10.4095/291946

Recommended citation:
Chung, C., Franklin, J.M., Dubé, B., and Hillary, E.M., 2012, Methodology for Assessing Prospectivity for Gold Deposits in the Canadian Shield. Geological Survey of Canada, Open File 7264, 64 p. doi:10.4095/291946

Methodology for Assessing Prospectivity for Gold Deposits in the Canadian Shield

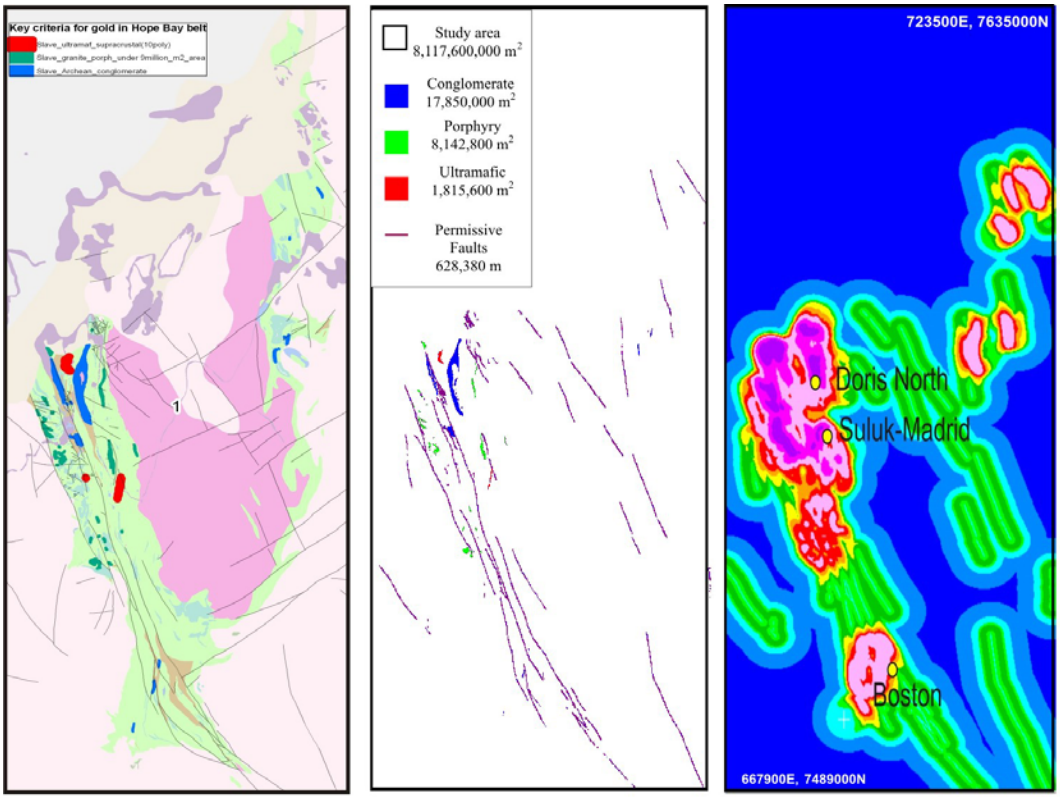

Chang-Jo Chung, James M Franklin, Benoît Dubé, and Elizabeth Hillary

March 2012

Methodology for Assessing Prospectivity for Gold Deposits in the Canadian Shield

Introduction

This work was performed for the Geological Survey of Canada under contracts #MGM031175W and #MGM031213W.

Following the development of a methodology for assessing the potential for discovery of volcanogenic massive sulfide deposits (Chung al., 2010), Dr. John Percival of Natural Resources Canada's Geological Survey of Canada (GSC) asked us to investigate the possibility of developing similar methodology for assessing the discovery potential for orogenic or "greenstone-hosted quartz-carbonate vein type" gold deposits in the Northern Canadian Shield. The approach for this evaluation is somewhat similar, using a set of key criteria derived from the well-established model for the formation of this broad class of gold deposits, and examining a digital map database for the presence of these criteria. A set of uncertainties were assigned to each criterion, based on the certainty of the identification of any criteria, as well as on the uncertainty of the value of any specific criteria to the model. Also, as for the VMS evaluation, "decay curves" were established for each criterion. Using these, the value of the observation of each criterion is diminished as a function of the distance from its observation.

Shield gold deposits have generally been assigned to a broad class of "orogenic gold" deposits that are distributed along crustal-scale fault zones formed during a major period of compressional to transpressional deformation that typically followed the deposition of volcano-sedimentary complexes in arc and back-arc-like settings (Dubé and Gosselin, 2007). The fault zones commonly (but not always) occur at the juxtaposition of major "domains" or sub-provinces. This type of gold deposit commonly is structurally controlled, with gold occurring in simple to complex networks of gold-bearing, laminated quartz-carbonate fault-fill veins in moderately to steeply dipping, compressional brittle-ductile shear zones and faults, with locally associated extensional veins and hydrothermal breccia zones. The veins occur in a broad variety of host rocks, although mafic and ultramafic volcanic rocks and competent iron-rich tholeiitic gabbroic sills and granitoid intrusions are common hosts (Dubé and Gosselin, 2007). District-specific lithological associations acting as chemical and/or structural traps for the mineralizing fluids are common as illustrated by tholeiitic basalts and flow contacts within the Tisdale Assemblage in Timmins (cf. Hodgson and McGeehan, 1982; Brisbin, 1997).

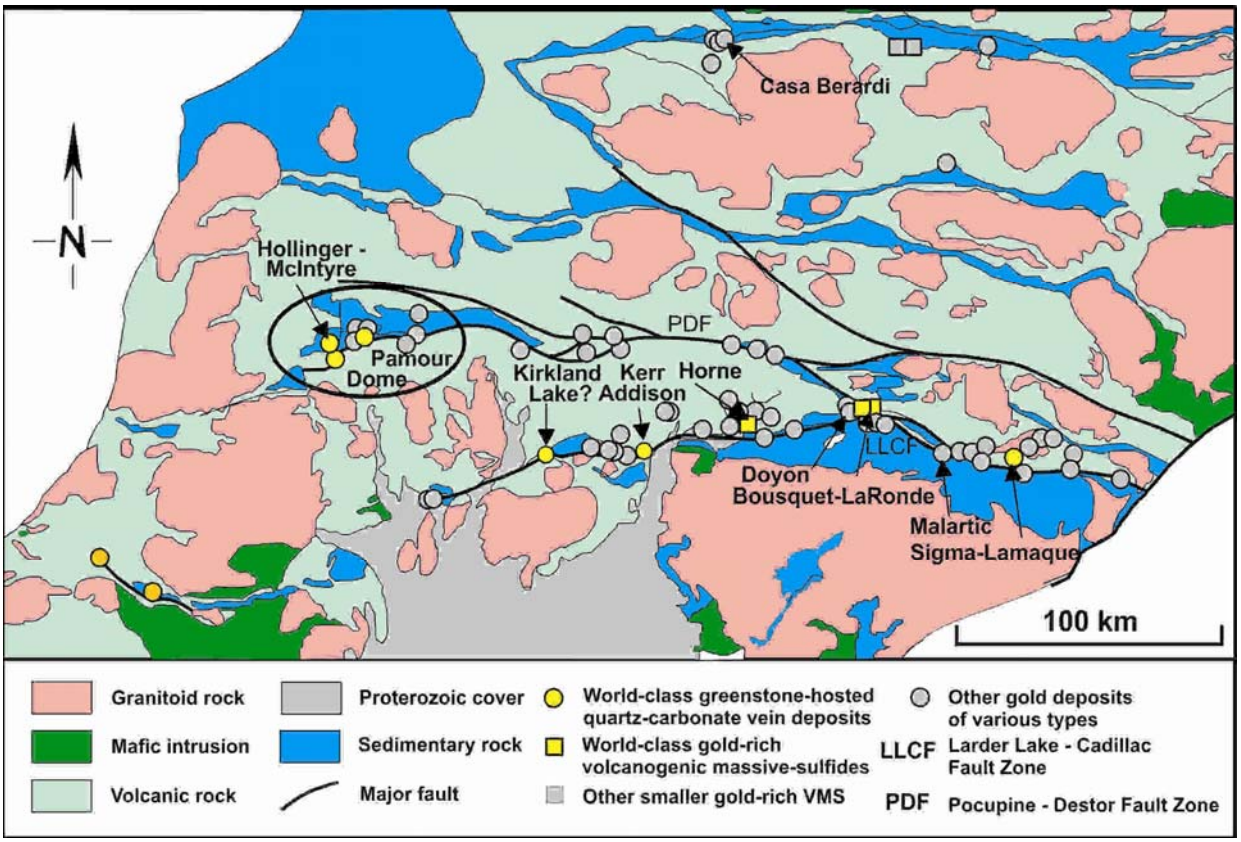

Figure 1: Geology and location of major gold deposits in the eastern Abitibi belt, Superior of the Canadian Shield; modified from Dubé and Gosselin, 2007

In contrast to volcanogenic massive sulfide (VMS) and other deposit types such as magmatic Ni-Cu, the orogenic or greenstone-hosted quartz-carbonate vein type has more complex genetic modes that remain the subject of debate (e.g. Goldfarb et al., 2005; Robert et al., 2005; Dubé and Gosselin, 2007). As a group, the orogenic deposits have many common attributes. Thus, in evaluating the criteria that we will use for our test, we chose attributes that are most commonly observed in association with the deposits, but some of them are empirical and not necessarily fully understood in the context of the genetic processes that attended gold deposition. Shield-related gold deposits are discussed extensively in various summary reviews (Poulsen et al., 2000; Goldfarb et al., 2005; Robert et al., 2005, Dubé and Gosselin, 2007 and references therein) and the key characteristics used in this study are provided in Table 1. These characteristics are based principally on their recurring presence in or near productive districts. Some have a well-understood genetic link to the deposits, whereas the genetic underpinning of others is more tenuous. There are many additional attributes that are found in the majority of gold-bearing districts that are not consistently reported in the databases that underpin the geological compilation maps that were used for this study.

The most extensively studied greenstone-hosted quartz-carbonate vein gold districts in the Canadian Shield are in the Timmins and Val D'Or camps (Figure 1). Deposits in the Kirkland lake camp are somewhat different, and although spatially associated with a major transpressive fault system, also have geochemical characteristics indicative of a magmatic genetic affiliation. Excellent compilation maps prepared by the provincial geological surveys were used to develop our methodology for this study (Ayer et al., 2004; Lamothe et al., 2005).

The first criterion, long-lived, compressional, crustal-scale faults, are present in virtually all gold districts. They are generally sub-parallel to the principal strike of the supracrustal units adjacent to them, and the amount of strain in these supracrustal rocks typically increases towards them. Few of these first order major faults contain large gold deposits. Exceptions include the Kerr Addison and Lapa gold deposits hosted within the Larder Lake-Cadillac Fault Zone. Most other deposits occur in and/or are associated with second- and third-order compressional reverse-oblique to oblique brittle-ductile high-angle shear zones commonly located within 5 km of the first order major fault, and best developed in its hanging wall (Robert, 1990, Dubé and Gosselin, 2007). Most of these complex and protracted regional-scale fault systems are accompanied by extensive hydrothermal carbonatization; this feature is particularly prevalent in large districts. Unfortunately, although usually noted on detailed (1:50,000 scale) maps, carbonatized zones are

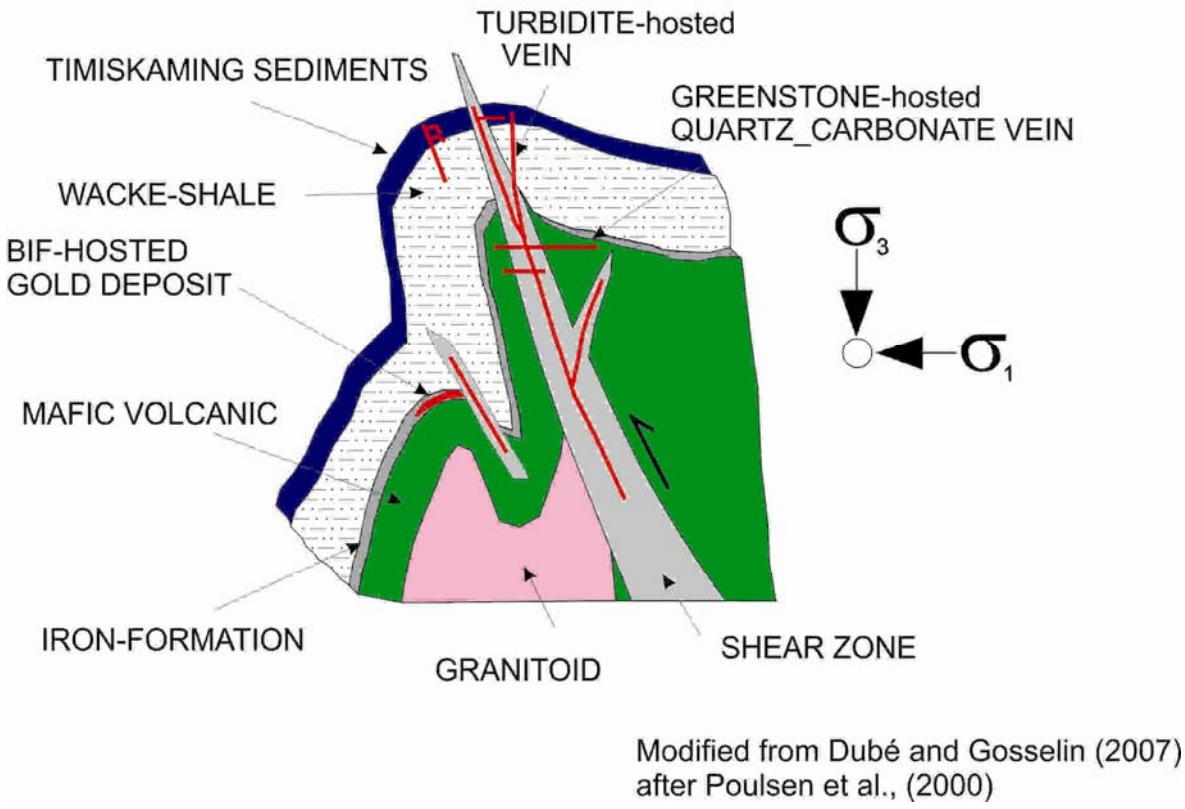

Figure 2: Schematic cross section of a typical setting of most vein- or "orogenic' gold deposits in the Canadian Shield.

not shown on most compilation maps. Overall, the major compressional to transpressional crustal-scale fault zones are considered to be the pathway towards higher crustal levels of speculatively gold-bearing metamorphically-generated fluids derived from prograde metamorphism and thermal re-equilibration of subducted volcano-sedimentary terranes during accretionary or collisional tectonics (cf. Kerrich et al., 2000 and references therein). Bends or "jogs" along major fault zones may be excellent loci for gold deposition, as these provide local dilation, causing disproportionation of $AuHS^{-}$, the principal gold-transporting complex, through sudden variation in fluid pressure and/or interaction with oxidizing mineral assemblages.

Many of the other features of gold-vein districts are shown in Figure 2. These illustrate almost all of the remaining key criteria (2-8) in Table 1. First, there is an empirical spatial, temporal and potentially genetic (?) relationship between large gold deposits and a Timiskaming-like regional unconformity (Dubé et al., 2003; Robert et al., 2005; Dubé and Gosselin, 2007). These Timiskaming-type sedimentary basins, commonly filled with conglomerate represent a first-order exploration target that commonly host part of the mineralization, as illustrated by large gold districts such as Timmins and Kirkland Lake (Poulsen et al., 1992; Hodgson, 1993; Dubé et al., 2000, 2003 and 2004; Robert et al., 2005, Dubé and Gosselin, 2007).

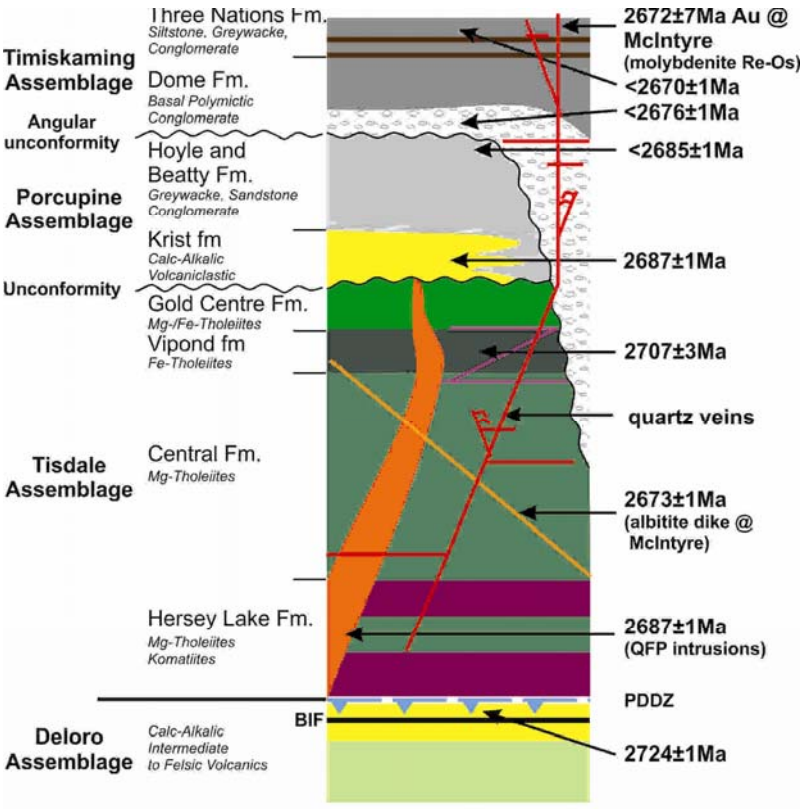

Figure 3: Composite lithostratigraphic assemblage in the Timmins area, Ontario (after Houlé et al., 2008).

The second feature (#3 in Table 1) is the presence of ultramafic bodies; these are typically komatiite flows, but also include subvolcanic mafic-ultramafic sills. These also have no direct genetic relationship to the presence of gold. The komatiites are commonly present in the lower portion of the stratigraphic succession and are juxtaposed against high-Fe tholeiitic strata (#4 in Table 1), in some of the largest gold district such as Timmins and Red Lake. They are typically highly altered (carbonatized with green micas) and deformed. Gabbroic sills, prevalent in some districts, are Fe-rich and rather competent units and as such constitute the preferential host of large deposits. Examples include

the Golden Mile dolerite sill in Kalgoorlie, Australia. Feature #5 in Table 1, felsic to intermediate shallow level porphyry dyke swarm or stocks and syenite bodies (depicted as "granitoid" in Figure 2), are also recurring features in gold camps. These intrusions commonly occur along major fault zones and consequently are spatially associated with greenstone-hosted quartz-carbonate vein deposits (Robert, 2001). They also commonly host at least part of the gold mineralization. Compositionally they range from quartz-feldspar porphyritic (typical of Timmins and Geraldton) to dioritic (Val D'Or) intrusions. In some camps (e.g. Kirkland Lake) alkaline intrusions and associated volcanic rocks are present. In the latter case, the volcanic rocks are associated with conglomerate, and are considered part of the "Temiskaming" assemblage. In the Timmins area, cross-cutting relationships combined with U-Pb geochronology have ruled out any direct genetic relationship between major gold mineralization and quartz-feldspar porphyry (e.g. Dubé and Gosselin, 2007). However, a genetic relationship remains possible for the syenite-hosted deposits such as Kirkland Lake (e.g. Robert, 2001; Ispolatov et al., 2008). Regardless of the role played by these intrusions, their unique presence in these camps makes them an important empirical guide.

Feature 6 (Table 1), banded iron formation (BIF), is typical of about 12% of Canadian Shield gold districts (e.g. Geraldton, Musselwhite, several Rae-Hearne and Slave districts). Its role is strictly as an oxidizing reactant for gold-bearing fluids. Typically, where shear-related cleavage transects tight to isoclinal fold noses in relatively brittle BIF, gold, pyrite and/or pyrrhotite and arsenopyrite are commonly precipitated, forming structurally controlled stratabound sulphide-rich replacement zones. In the giant Timmins camp, for example, where all major deposits occur north of the main Destor-Porcupine fault zone, BIF is a common lithology south of the fault but contains only small gold occurrences.

Feature 7, dyke swarms, albitite, and lamprophyre are late-stage igneous tectonic features, in some cases petrogenetically related to the porphyry dykes described in Feature 5. The genetic relationship between such intrusions and gold is variable and controversial but they commonly have a close temporal relationship, and tend to occupy the same major structures as the gold vein systems. These may occupy the same deep penetrating conduits as the gold-bearing fluids. This is illustrated by lamprophyre intrusions in Red Lake (e.g. Dubé et al., 2004). In Timmins, the albitite dykes cut feldspar porphyry intrusions and are themselves cut by gold-bearing quartz-carbonate quartz veins.

Finally, Feature 8 is a less evident feature at a map scale, and thus was not used in this classification system. However, some gold districts occur at the boundary between greenschist and amphibolite assemblage strata. Deposits in most districts occur in greenschist terranes, but a few notable exceptions (e.g. Lupin, Musselwhite) are in amphibolite-assemblage strata.

	Criterion/Sub-criterion	Notes	Weighting factor	Maximum Distance	Likelihood of Correct Identification
1	Long-lived compressional Crustal scale fault (50-100km long)		1	6000	0.9
		· (30-50 km spacing between gold camps along fault zone)			
		· 80% of gold in 20% of the deposits			
	sub-criteria: curvature/jog/bend or second and third order faults/shear				
2	Unconformities/Timiskaming-like fluvial-alluvial conglomerates		0.8	6000	0.8
		· disconformities between mafic-ultramafic rocks and coarse clastic sediments distributed along major fault zones or defining/masking major fault zones(large deposits are near unconformities-regional contact)			
		· unconformity between mafic-ultramafic volcanic and overlying coarse clastic sequence			
	sub-criteria: folded unconformities				
3	Ultramafic flows in lower stratigraphic succession		0.4	6000	0.8
	sub-criteria: green-carbonate rocks/iron-carbonatized ultramafic with green micas				
4	Fe-rich tholeiitic basalts (variolitic)/differentiated gabbroic (dolerite) sills		0.8	100	1
	sub-criteria: folded contact between basalt and ultramafic/komatiite basalt				
5	Felsic-intermediate shallow level porphyry dyke swarm or stocks and syenite		0.6	6000	0.7
		Emplaced along unconformities or major faults commonly lacking in BIF-hosted gold deposits			
6	Regionally extensive Banded Iron Formation		0.4	1000	1
	sub-criteria: folded/intersected by faults-shears/				
	sub-criteria: near mafic volcanic contact				
	sub-criteria: low magnetic intensity				
7	dyke swarms, albitite, lamprophyres injected in fault zones		0.5	500	
		· implies deep structures tapping fluid(s)			
8	Greenschist facies to lower amphibolite		0.5	100	0.9
	sub-criteria: greenschist facies-lower amphibolite transition				

Table 1: Key geological characteristics (“Key Criteria”) of vein-gold deposits in the Canadian Shield

The composite lithostratigraphic assemblage for the Timmins area illustrated in Figure 3 (Houlé et al., 2008) serves to summarize the key features of a major gold-bearing district. The major regional-scale structural zone, the Destor Porcupine fault zone (PDDZ in Figure 3) separates two assemblages that are remarkably different in composition and age (2724Ma south of the fault, <2669Ma north of it), and further illustrates that all of the BIF is south of the fault. The Tisdale Assemblage contains abundant ultramafic rocks juxtaposed against tholeiitic lavas, providing the type of ductility contrast that typifies some of the most productive camps. The Tisdale is cut by several QFP dykes and stocks, and locally contains albitite dykes. Its upper portion consists of Fe tholeiite (Vipond Formation), a brittle and Fe-rich reactive rock that host part of the gold vein systems. The upper part of the Tisdale, as well as the unconformably overlying Porcupine Assemblage (volcaniclastic and wacke-dominant) strata are themselves unconformably overlain by a distinctive conglomerate unit of the Temiskaming Assemblage. This unconformity and conglomerate-filled basin is an excellent representative of the late-Archean extensional basin assemblage noted in Feature 2 (Table 1).

Note that all coordinates shown on the following maps are in NAD83: Zone 12 for Slave Province and Zone 17 for the Abitibi regions.

A) Procedure for obtaining "permissive faults" for gold deposits

The first of the ***Key criteria*** (Table 1) used to identify areas with good potential for the discovery of gold deposits is the presence of "***permissive faults***", those major, district-scale transpressive structures that occur in virtually all gold-bearing districts. *Permissive faults* are defined as the faults that are sub- parallel to the contacts of the volcanic strata in each greenstone belt. Given that to construct our methodology we must not assume any prior knowledge of the location of gold deposits or the most relevant fault systems, we had to establish a method for identifying permissive faults on the basis of their relationship to the general strike of the strata in the areas under examination. To obtain the permissive faults systematically in each greenstone belt, we have used the following four-step approach. For each greenstone belt:

(Step 1.1) Generate a ***volcanic contact data layer*** where the contacts between volcanic strata are identified from the geological map. Compute the angle of the tangent of a point on the contacts. To obtain the tangent, we have used the following procedure: Consider a point on the contact. Define the length of a unit vector, such as 200m, depending on the map scale. Fit a unit vector along the contacts such that the midpoint of the unit vector lies on the point. The fitted unit vector is considered the "tangent" of the contact at the point. Compute the angle of the vector. Repeat the procedure along the volcanic contact by moving the point a short distance such as 20m. Obtain all the angles of the unit vector-tangents. Generate an empirical frequency distribution function of the angles of the unit vectors along the volcanic contacts. Areas selected for evaluation should have only one prominent strike direction (i.e. unimodal strike distribution, +/- 20^{o}). This is generally the case for major greenstone belt segments such as the Timmins, Kirkland Lake or Val d'Or

areas, but individual greenstone belt within large areas, such as individual volcano-sedimentary domains in Slave Province, should be examined separately.

(Step 1.2) From the empirical frequency distribution function, identify the ***narrowest ranges of the angles*** containing approximately 50% of the unit vectors (tangents).

(Step 1.3) Generate a ***fault data layer*** containing the all faults. Compute the angles of the tangents of the points on the faults by following the same procedure described in **Step 1.1**.

(Step 1.4) Select all unit vectors - tangents of the faults whose angles are within the narrow range identified in **Step 1.2;** i.e. faults that are subparallel to the volcanic contacts. These selected unit vectors constitute the "***permissive faults***" for gold deposits.

We illustrate this four-step approach by using the data from the Hope Bay greenstone belt, Nunavut. The contacts of volcanic rocks in the Hope Bay belt are shown in Figure 4(A).

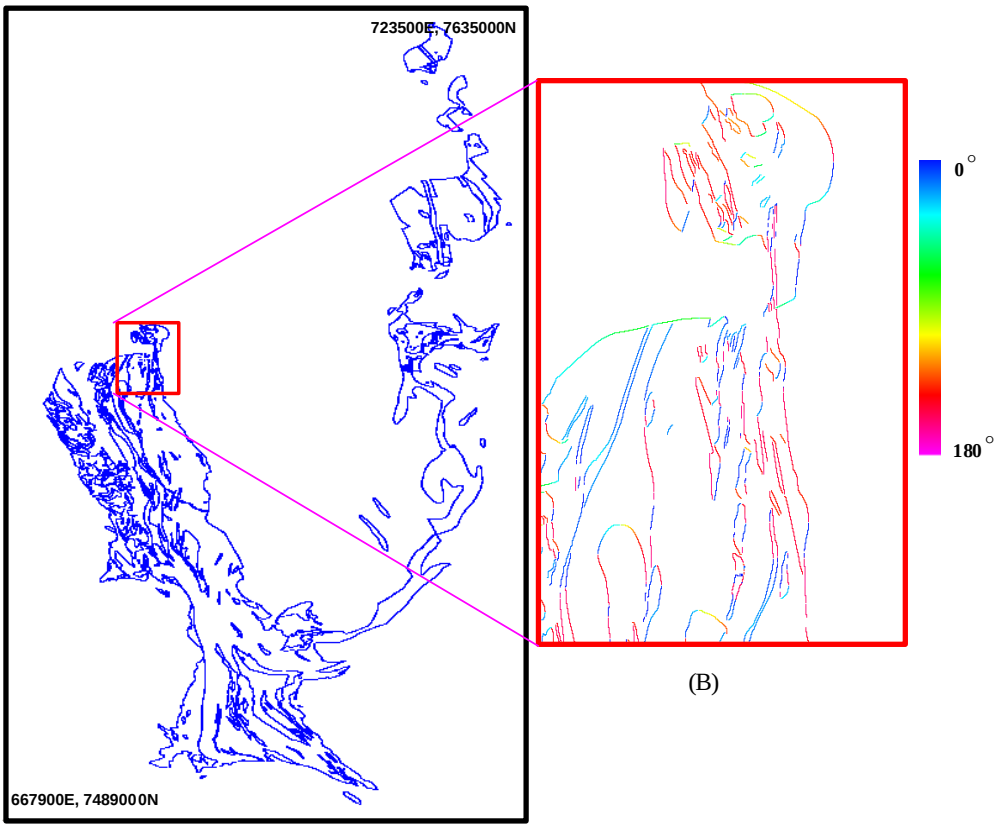

Figure 4: (A) Contacts of volcanic rocks in Hope Bay greenstone belt. (B) The angles of the tangents to the contacts in a subarea bounded by red rectangle in (A), ranging from 0^{o} to 180^{o}. Coordinates for the adjacent corner of each diagram are in UTM (NAD83 Zone 12).

Following the procedure in **Step 1.1**, the angles of 132,474 tangents at every 20m along the volcanic-contacts (the total length of all volcanic contacts is 2,649.480 km) were computed. The empirical frequency distribution function using an estimated 132,474 angles is shown as a blue curve in Figure 5.

As defined in **Step 1.2**, we obtained the range 140° to 179.5° as the shortest range of angles containing approximately 50% of the tangents to the volcanic contacts for the Hope Bay belt. Colour coded angles of the tangents to faults for a small portion of the Hope Bay belt (red rectangle in Figure 6A) are illustrated in Figure 6B. The permissive faults were generated by selecting faults whose tangents lay within the range 140° to179.5° (Figure 7), as defined by the volcanic contacts (Figure 4B).

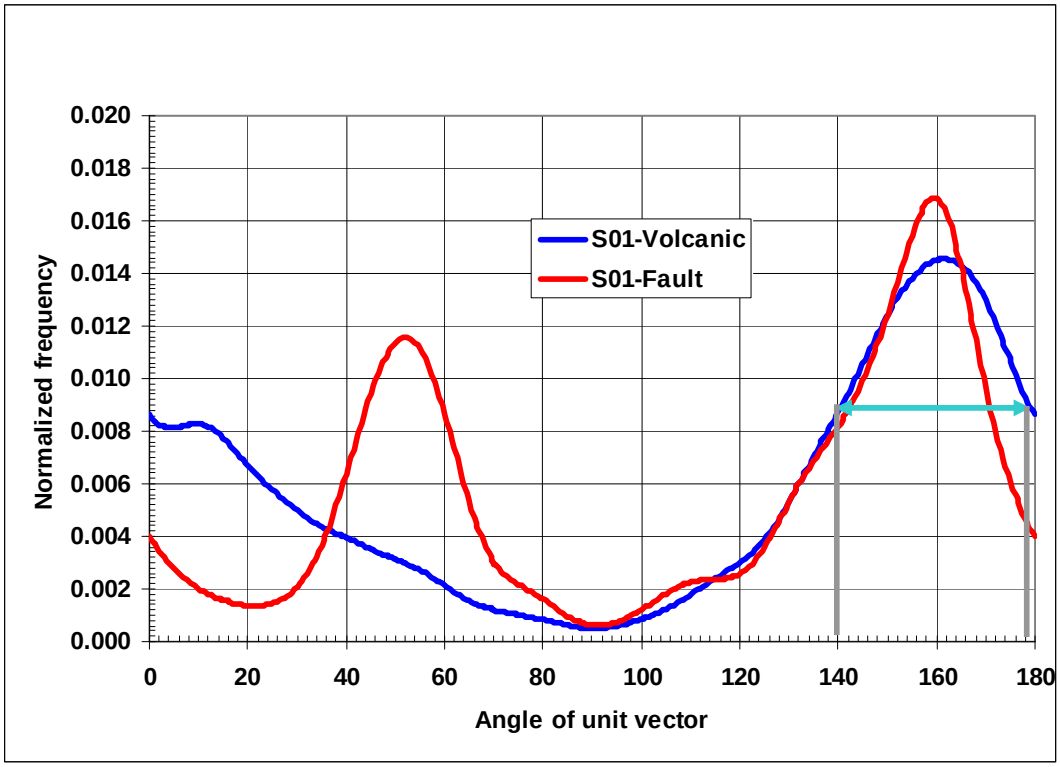

Figure 5: Empirical frequency distribution function for the angles of the tangents to the contacts of volcanic rocks shown in Figure 4 in the Hope Bay greenstone belt is shown as blue curve. The empirical distribution function is based on 132,474 tangents computed at 20m intervals along the contacts. The shortest range of the angles containing approximately 50% of the tangents is 140° to 179.5°, illustrated by two gray bars with turquoise arrow. An empirical frequency distribution function of the angles of the faults is illustrated as a red curve (based on 69,376 tangents to the faults).

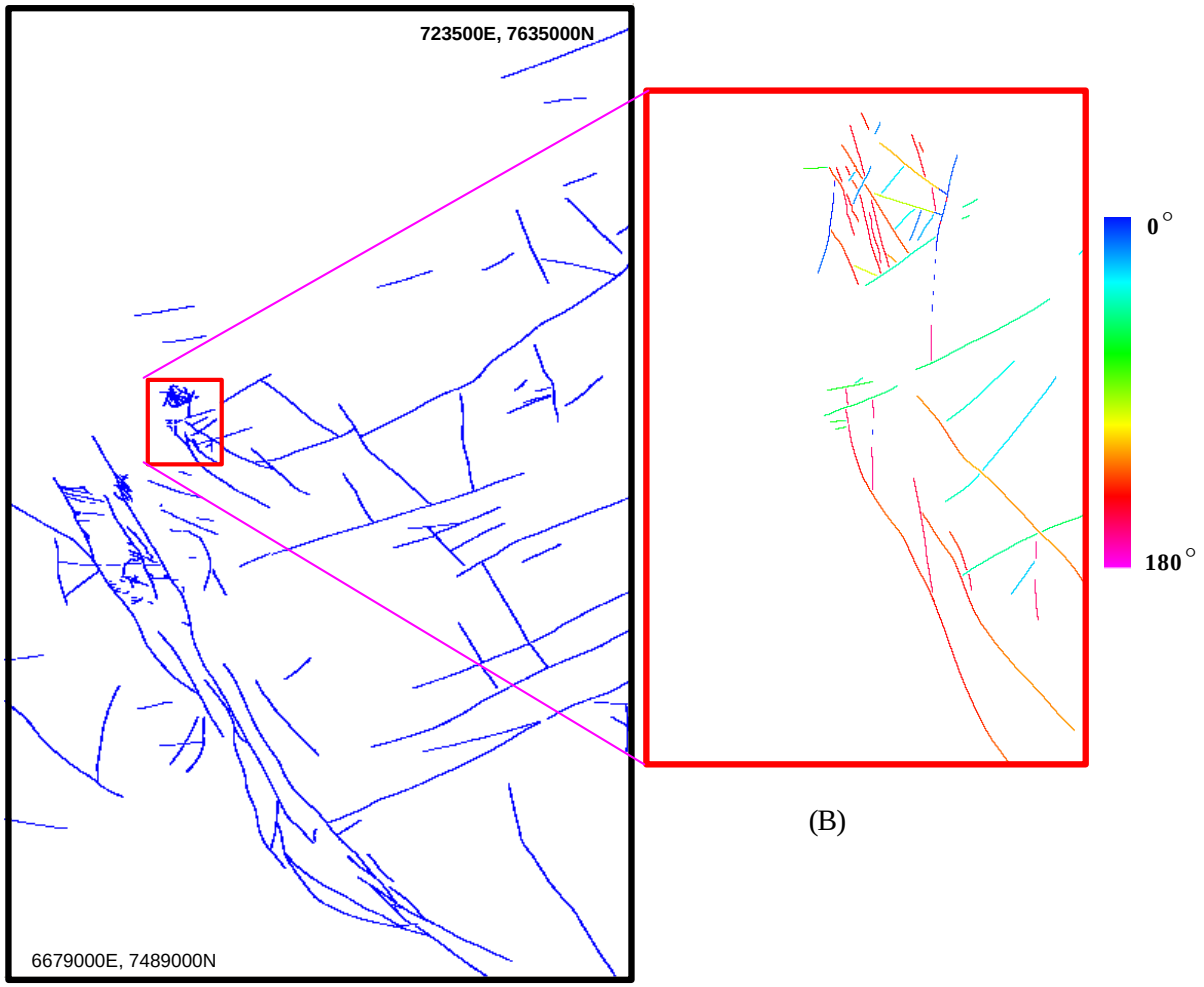

(A)

(B)

Figure 6 (A): Faults in Hope Bay greenstone belt. (B): The angles of the tangents to the faults in a subarea bounded by red rectangle in (A) are shown. The angles of the tangents range from 0 to 180.

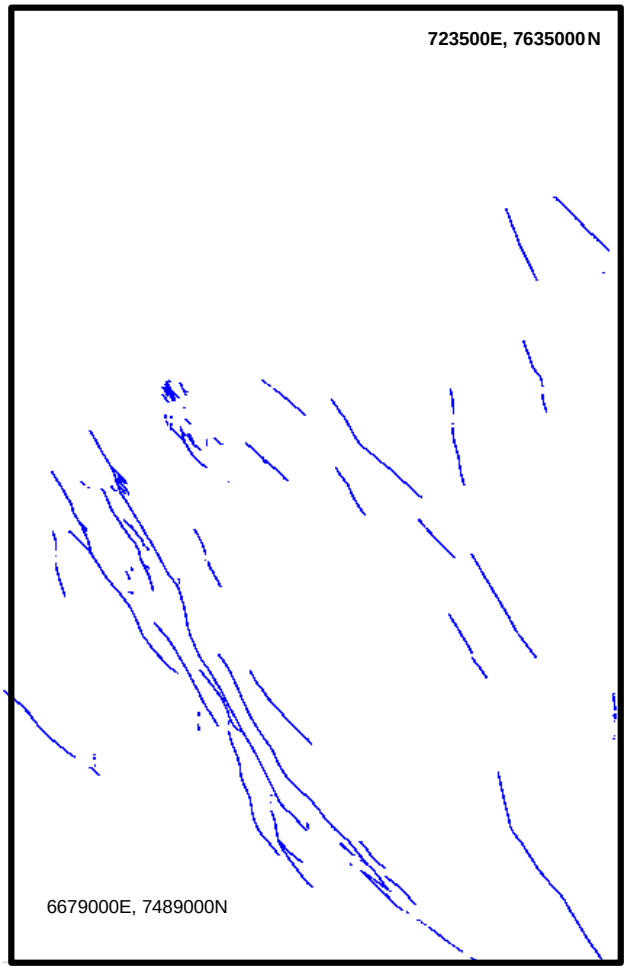

Figure 7: Permissive faults for gold deposits in Hope Bay greenstone belt. The permissive faults were generated by selecting faults whose tangents lay between 140° and 179.5° to the contacts of volcanic rocks. This range contains approximately 50% of the faults that are tangent to the contacts of volcanic rocks. Coordinates are UTM values (NAD83 Zone 12).

B) Generating decay (favourability) functions and potential map

The ***"Key Criteria" related to the discovery of gold deposits*** in any selected area are summarized in Table 1. In addition to the permissive faults, we consider only four additional geological units because of limited information available from small-scale maps such as 1:500,000 map-scale. These additional criteria include the presence of: 1) mafic volcanic rocks, 2) Timiskaming-like

clastic sediments (i.e. conglomerates), 3) small porphyritic, granitoid or alkaline late-tectonic intrusions within the greenstone belts, and 4) supracrustal ultramafic rocks. For simplicity, these

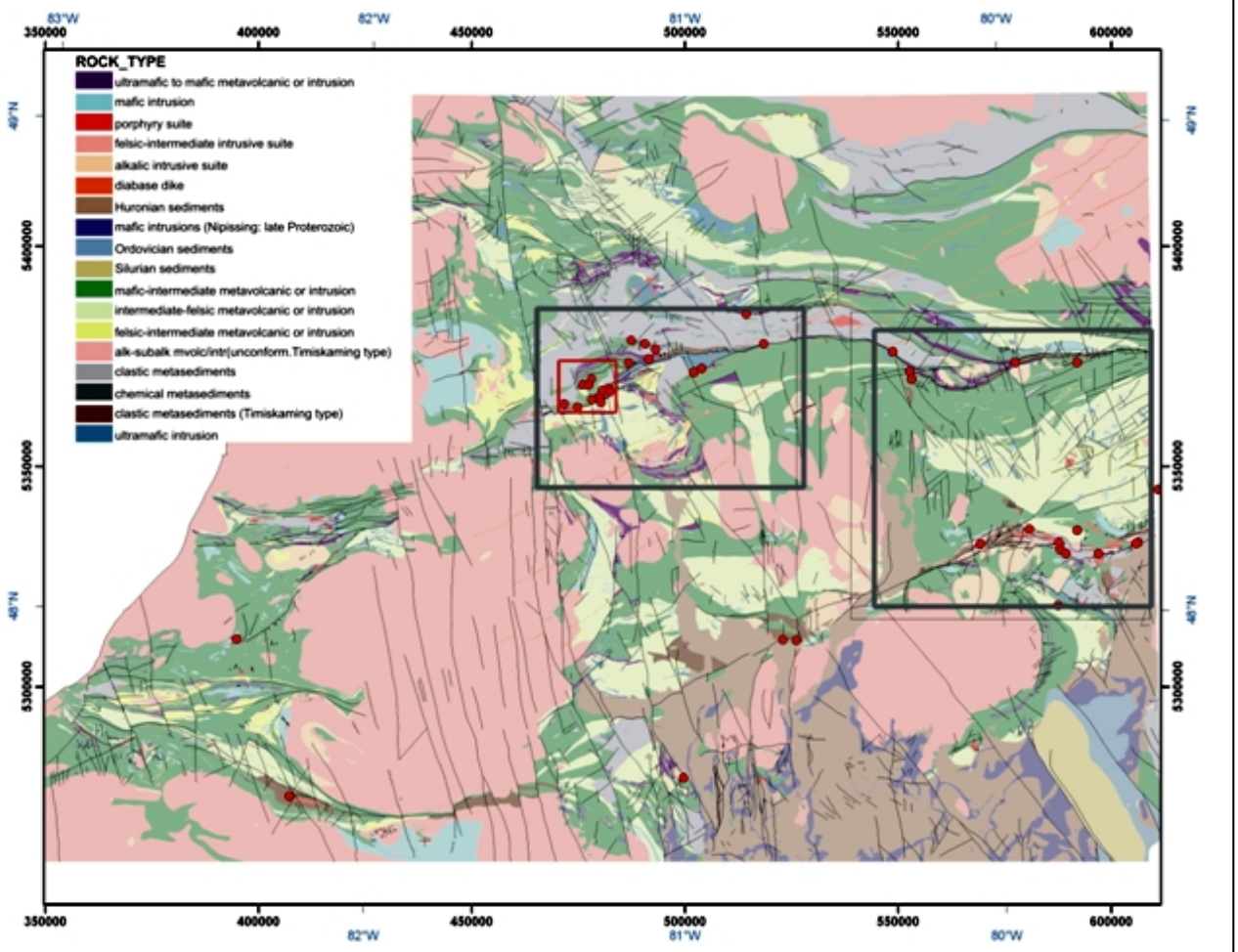

Figure 8: Geology map of Abitibi area, Ontario (after Ayers et al, 2004).Red box includes area for Figure 9 (below), which includes the two largest gold deposits in the Abitibi belt. Boxes outlined in grey enclose the three main gold camps in the Ontario portion of the Abitibi belt. These are used as test areas for the methodology. Coordinates are UTM values (NAD83 Zone 17) in black, and latitude-longitude values in blue.

units will be referred to in this document as “mafic volcanics”, “Timiskaming sediments”, “intrusions” and “ultramafics”. We will illustrate the procedure using a small subarea (red box) of the Abitibi map in Figure 8, which contains two of the largest gold deposits in the Abitibi area: Hollinger with 986 tonnes ((31,700,886 troy ounces) and Dome with 508 tonnes (16,332,708 troy ounces). The larger grey rectangles outline test areas referred to in subsequent sections. The overall geology and location of the main geological criteria for our study are shown in Figure 9A and 9B.

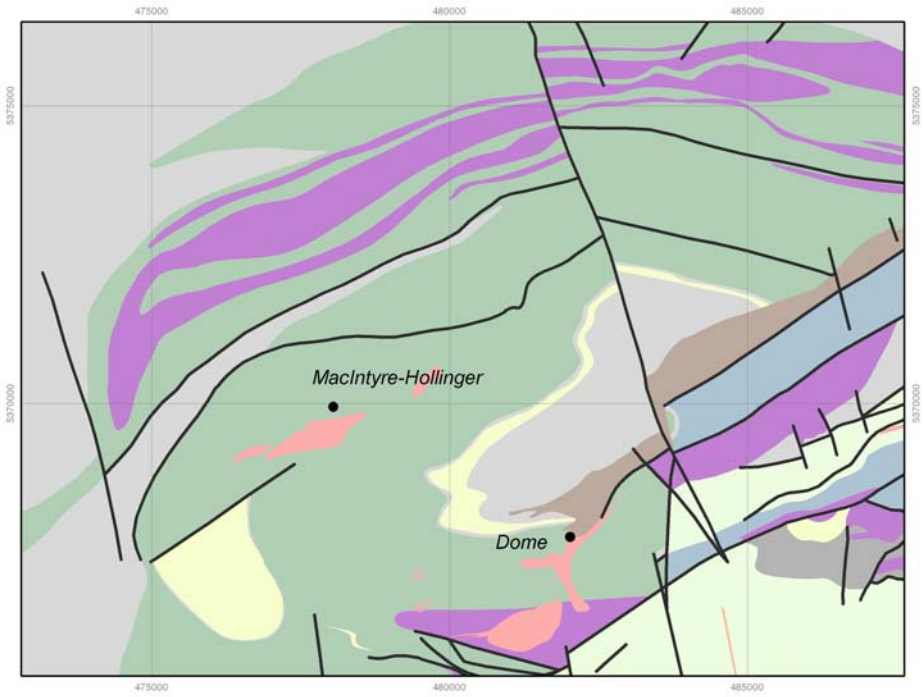

Figure 9A: Detailed geology in Hollinger-Dome area, defined by red box, Figure 8 (after Ayer et al, 2004); legend as in Figure 8. Only the two largest deposits are shown. (UTM NAD83, Zn17).

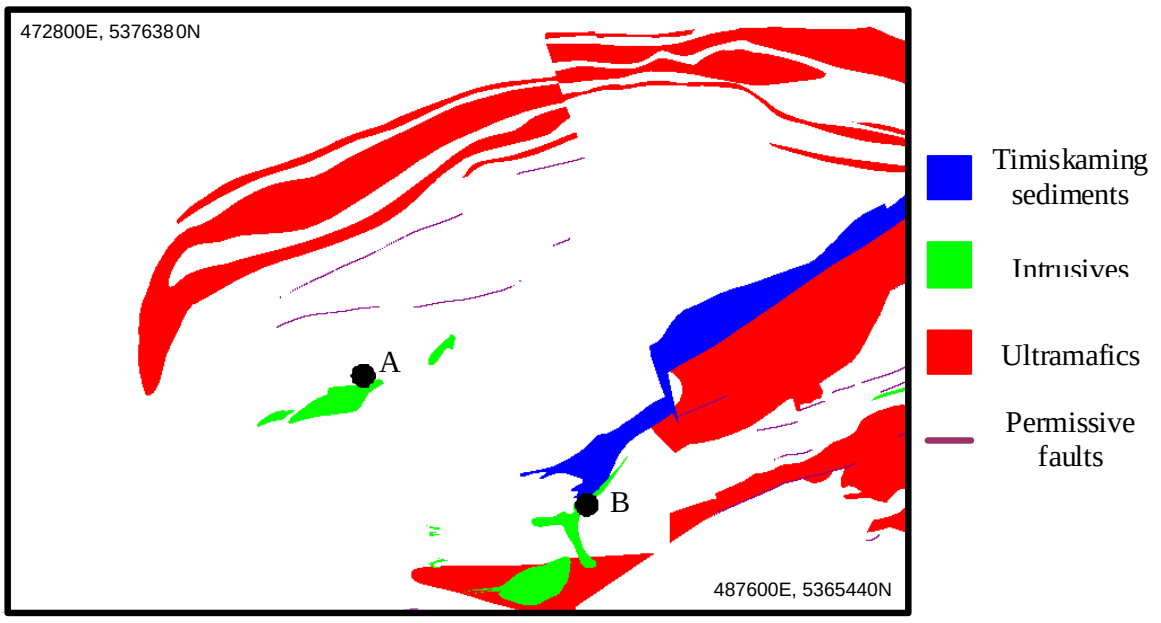

Figure 9B: Permissive faults and main geological criteria near two largest deposits in Timmins greenstone belt (UTM NAD83, Zn17).

Using the criteria without modification for an estimate of their reliability, determining an absolute measure of the "***probability (or certainty)***" of the next gold discovery for any specific map area would be less certain. However, each criterion will provide a measure of the "***relative significance or favourability***" with respect to the existence of gold deposits in an area. An attempt has been made to convert the presence of or proximity to key criteria to a mathematical function such that we can generate a measure of the relative favourability with respect to the potential existence of the gold deposits in the area.

The conversion to a mathematical form is achieved in three steps. The first two steps transfer each key criterion into a mathematical function. Using a rasterized geology map, in which each pixel is assigned the underlying lithology as shown in Figure 9B, we then, on a pixel-by-pixel basis, evaluate the distance from any pixel to the nearest presence of a pixel that contains a key criterion.

(Step 2.1) to generate a *data layer* where each value at a pixel (pixel value) is a value for the shortest distance to a specific criterion as illustrated in Figure 10 for Timiskaming sediment (black polygon in Figure 10).

(Step 2.2) to develop a mathematical model that estimates the relative favourability for the discovery of the gold deposits as a function of the distance from an observation point (pixel) to the nearest pixel that contains that criterion as generated in **(Step 2.1)**. This function usually describes the non-linear relationship between the value of the likelihood of discovery of the gold deposit and its distance away from that key attribute.

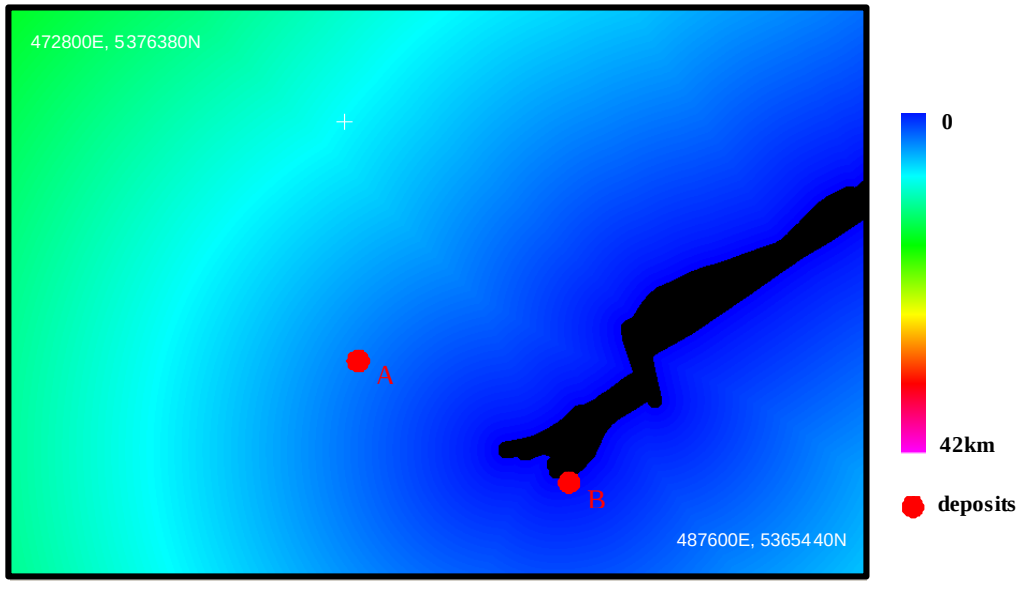

Figure 10: Contour map illustrating the proximity (km) to Timiskaming sediments (in black). Two red dots A and B represent Hollinger and Dome gold deposits as in Figure 9 (UTM NAD83, Zn17).

The mathematical function in (Step 2.2) is termed the "decay function", determined for each of the key criteria for gold deposits (from Table 1). Its values range from 0 to 1. Through the decay function, each pixel value in the data layer (map) generated in (Step.1) is converted to a value between 0 and 1 depending on the relative significance (or favourability) for gold deposits. For example, as noted in Table 1, proximity to "Timiskaming-like" sediments does significantly (although not directly) relate to the presence of gold deposits. Most gold deposits are adjacent to these strata, not within them; hence the most favourable location is located "b" units away from the observation. If a pixel is located greater than 6000m from the nearest "Timiskaming-like" sediments, its value representing the relative significance for gold deposits will be 0. For each key criterion, one decay function is generated.

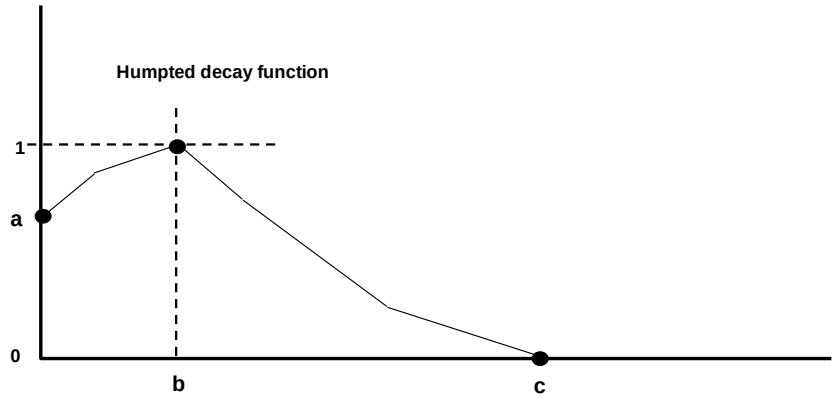

Figure 11: Graphical illustration of "humped decay function". Three parameters, a, b and c are required to establish the shape of a humped decay function. One decay function is required for each criterion for gold mineralization. X-axis represents the distance from geological unit (e.g. Timiskaming sediments) and the Y-axis shows a measure (value from 0 to 1) representing the relative significance or favourability for gold deposits.

We use these steps to generate a gold potential map for the Timmins - Kirkland area, Ontario. For the first criterion: the presence of "Timiskaming - like" sediment rocks in Table 1, we generated the first data layer, named "Timiskaming data layer", by computing the distance to the nearest Timiskaming strata from each pixel shown in Figure 7. The pixel values assigned to each pixel in the data layer represent the shortest distance to the presence of Timiskaming sediment rocks and these distance values range from 0 (presence of Timiskaming sediment rocks) to 42km within the whole Abitibi study area. The pixel values will be used to calculate the relative significance or favourability with respect to the existence of the gold deposits in the next step. The "decay function" to be established for the "Timiskaming sediment" criterion estimates the "favourability score" characterizing the "relative significance (or favourability)" for gold deposits as a function of the distances from Timiskaming sediments. As shown in Figure 11, a "humped" decay function was specifically formulated for this gold study to account for the most favourable distance being adjacent to (by distance "b"), but not in the sedimentary strata.

To establish a humped decay function, three parameters, a, b and c are required to define its shape. Three sets of the decay functions are considered as shown in Table 2. The first two sets are independent evaluations by two of the authors: the JF (James Franklin) model and BD

(Benoit Dubé) model. The third was modified from these, in consideration of the location of known deposits relative to the presence of each criterion in the test area.

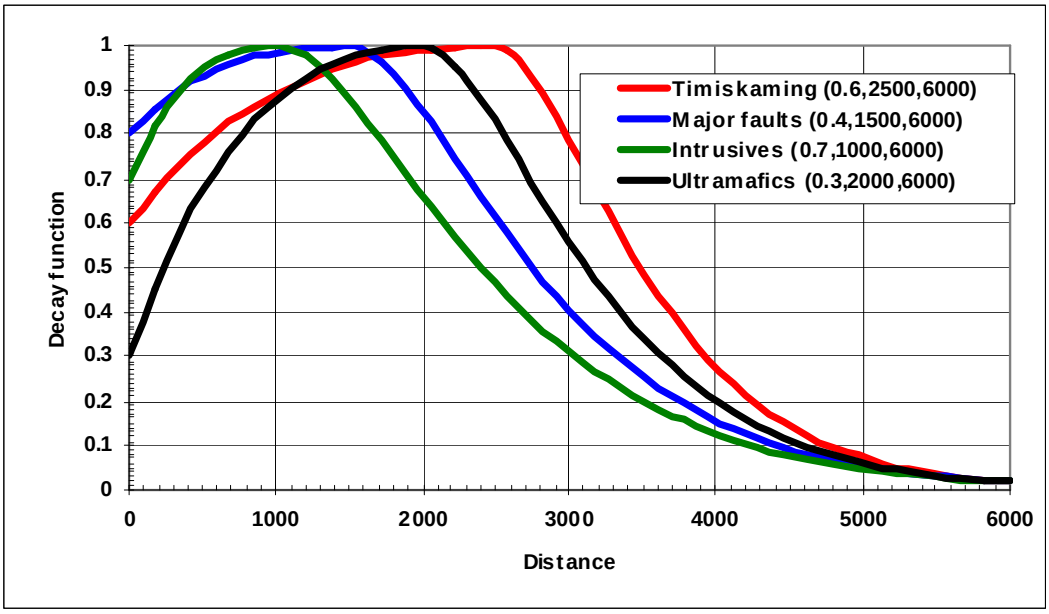

(A)

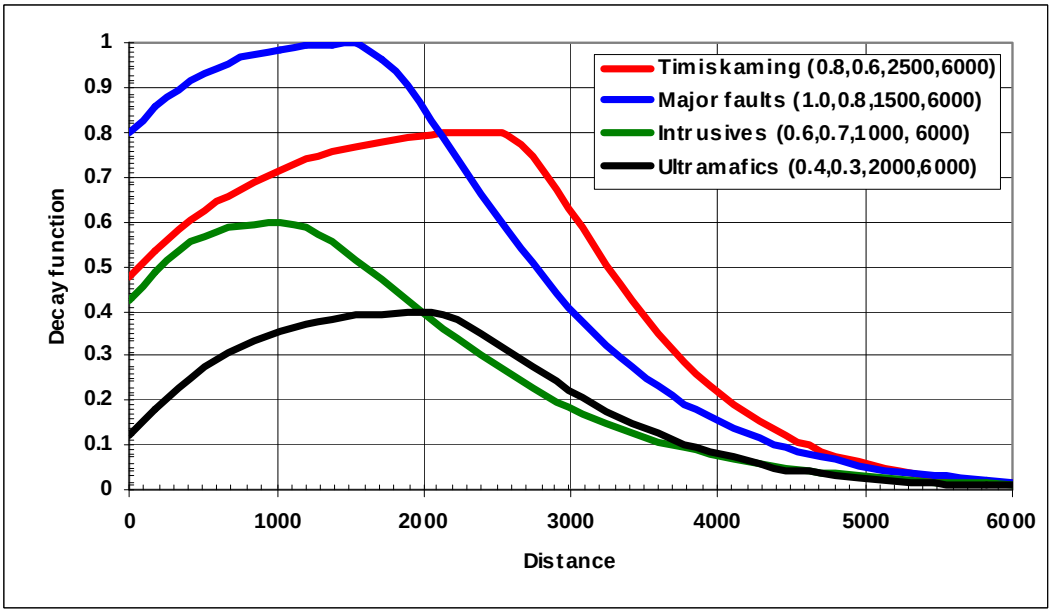

(B)

Figure 12. (A) Four unweighted "humped decay functions" based on four criteria, using three functions, a, b and c, to define the shape of each as provided in the "New Model" in Table 2. One decay function is required for each criterion for gold mineralization. (B) Four weighted decay functions were obtained from the four decay functions in (A) by using the four weights (measures of significance to the genetic model) shown in Column 1 in Table 2.

JF model

Weights	Uncertainty	a	b	c	
1.0	0.9	0.4	3000	6000	Timiskaming
1.0	1.0	0.0	1500	6000	permissive faults
0.8	0.8	0.8	200	4000	Intrusive
0.5	0.9	0.2	2000	6000	Ultramafic

BD model

Weights	Uncertainty	a	b	c	
1.0	0.9	0.8	2000	6000	Timiskaming
1.0	1.0	0.5	2000	6000	permissive faults
0.8	0.8	0.5	200	4000	Intrusive
0.5	0.9	0.3	2000	6000	Ultramafic

New Model

Weights	Uncertainty	a	b	c	
0.8	0.8	0.6	2500	6000	Timiskaming
1.0	0.9	0.8	1500	6000	permissive faults
0.6	0.7	0.7	1000	6000	Intrusive
0.4	0.8	0.3	2000	6000	Ultramafic

Table 2: Three set of decay functions are considered. The first two sets, JF (James Franklin) and BD (Benoit Dube) models are experience-based, and somewhat subjective. In addition to the three parameters a, b and c, two additional parameters, one for weights and the other for the "uncertainty" of the criterion, were also required to establish the criterion completely. One decay function is required for each criterion for gold potential. Four criteria were used to generate a potential map. The "New Model" was constructed by combining the first two sets of decay functions, and modified using the actual presence of gold deposits, and all subsequent experiments were performed using the decay functions in the New Model. Four decay functions based on the new model are illustrated in Figure 12(A).

The weights in the first column in Table 2 are included to express the relative importance of the corresponding criteria, and thus their decay functions. We have incorporated the weighting factor in the construction of the decay function as a multiplicative factor to that function, such that its maximum value is limited by the weighting factor. The weighting factors account for the criticality of each criterion to the presence of gold deposits, derived from consideration of the genetic model and extensive observation of many districts by the authors. The four weighted decay functions are shown in Figure 12(B). After a decay function is established using the three parameters that define its shape, a, b and c, it is weighted by multiplying the weighting factors (first column in Table 2). Note, however, that, the unweighted decay function for the "permissive faults" criterion (blue curve in Figure 12A) is the same as the corresponding weighted decay functions because its weighting factor is 1 (i.e. it is considered the most significant criterion of all).

One decay function is required for each criterion. Each weighted decay function in Figure 12(B) computes "***favourability score***" at each pixel for the corresponding criterion. For the Timiskaming criterion, the favourability score is computed by following the red curve in Figure

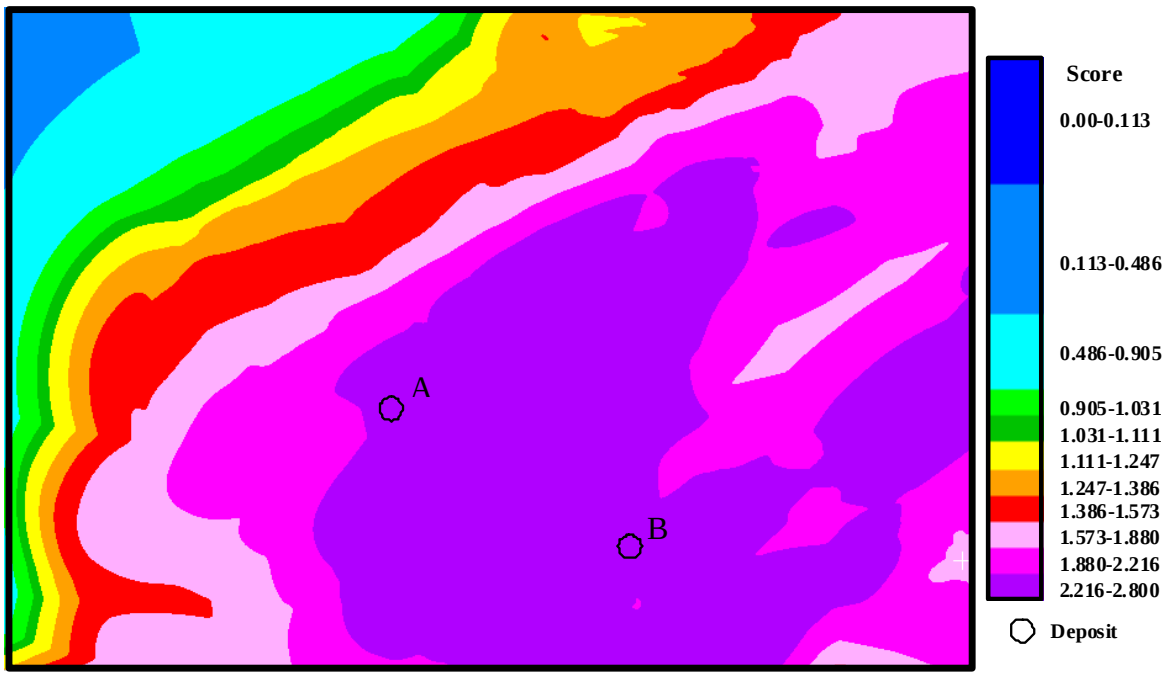

Figure 13: Using the distances from the permissive faults and the three geological units, Timiskaming sediments, intrusions and ultramafic bodies, this gold potential map near the two largest deposits in Timmins greenstone belt (see Figure 9 for coordinates) was generated, based on criteria 1, 2, 3 and 5 in Table 1. Black dots A and B represent gold deposits Hollinger and Dome, with 986 and 508 tonnes (31,700,886 and 16,332,708 troy ounces), respectively.

12(B) at each pixel. For example, consider the pixel (shown as "**A**" in Figures 9b and 10) that contains the largest deposit, with 986 tonnes of gold. It is located 3334m from the nearest Timiskaming sediments. Using the decay function for Timiskaming strata (red curve in Figure 12(B)), a favourability score of 0.532 is obtained. In addition, the pixel is also located 1150m, 100m and 2397m from the nearest "permissive faults", "intrusions" and "ultramafics", respectively. By following three decay functions, the blue, green and grey curves in Figure 12(B), we obtained three additional favourability scores 0.994, 0.465 and 0.364, respectively for the likelihood that the pixel contains a gold deposit.

At every pixel in the study area, based on the distances from the presence of the four criteria, four favourability scores are obtained using the four decay functions shown in Figure 12(B). There are many ways integrate these four scores into one value. In this study, we have simply computed the sum of these four scores at every pixel. The sum at every pixel generates a potential value for the potential for gold mineralization. For example, the sum score for the pixel that contains the largest deposit is 2.355, representing the relative likelihood of having a gold deposit at that pixel. Contouring the sum score of every pixel, a gold potential map was generated for Timmins-Kirkland Lake study area shown in Figure 13. Using the four decay functions shown in Figure 12(B), the maximum sum score 2.8 (=0.8+1+0.6+0.4) can obtained.

The representation of the relative significance or favourability for gold deposits by the decay function is based on the assumption that the presence of the 4 key geological units, Timiskaming sediments, permissive faults, intrusions and ultramafic units, are "true." However, in reality, the presence of the geological units as shown on a map or contained in the digital file may only be assumed to be true, and the positional and geologically interpreted accuracy of the key criteria depends to some extent on the scale of the geological map used, as well as the somewhat subjective interpretation of the geologist who mapped the area. The uncertainty or dependence on the accuracy of this boundary is represented in part by the number shown in the fourth column under the heading of "uncertainty" in Table 2. We will later use it to determine our uncertainty of the representation of a specific type of unit, which will in turn affect our estimation of the favourability for presence of gold deposits.

C) Test procedure for gold potential map in Timmins-Kirkland Lake area:

The contoured potential map (Figure 14), based on the sum score at every pixel, can be visualized several ways by slicing the scores. One of the most effective ways to visualize the potential map is by using a "*ranking*" procedure. When two pixels with two summed scores are considered, the pixel with higher score is more likely to host a gold deposit than the other pixel with lower score. This is because the favourability score measures a relative **significance for**

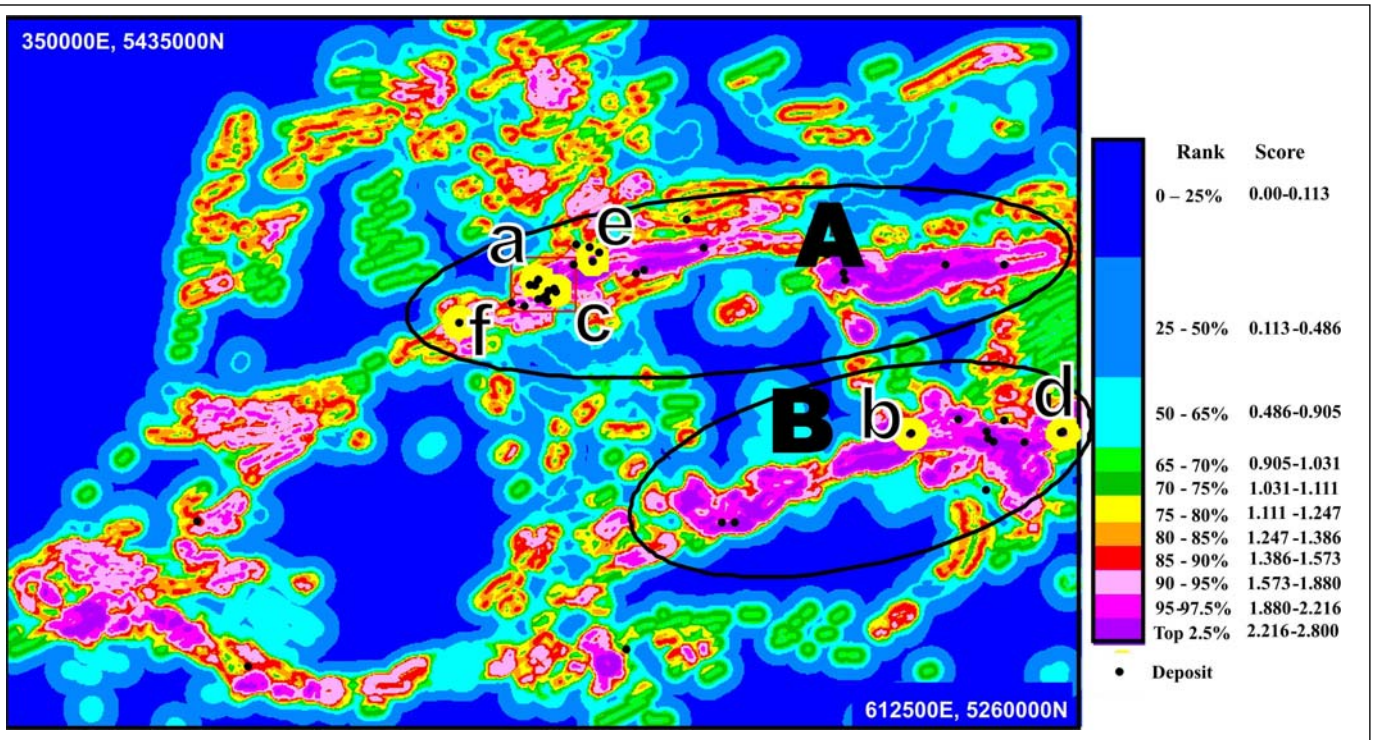

Figure 14: Gold potential map for the Timmins-Kirkland study area (same coordinates as geology map, Figure 5) based on the four criteria: permissive faults, Timiskaming sediments, intrusive and ultramafic units. The 39 black dots represent gold deposits containing more than 32,151 oz (1 tonnes) of gold. Among the 39 black dots, five yellow-circled dots indicate the largest five deposits with 986 (a), 797(b), 508(c), 327(d) and 249(e) tonnes of gold. Yellow-circled black dot (f) represents a newly discovered deposit. The Timmins-Kirkland study area consists of 45815 km^2. The range of scores is divided into 11 classes using the ranking procedure based on the sum scores computed. The highest potential area (dark purple) occupies 2.5% of the entire map sheet encompassing 1,145 km^2. The scores of the pixels range from 2.216 to 2.8. The next highest potential area (magenta) also occupies 1,145 km^2, where the scores range from 1.88 to 2.216. All five largest deposits are located within these two top potential areas. The order of potential is represented by pink (5%, 2,290 km^2), red (2,290 km^2), orange (2,290 km^2), yellow (2,290 km^2) and dark green (2,290 km^2). The colour legend also includes the ranges of the scores. Two areas enclosed by two black ellipses, **A** and **B** outline "Timmins greenstone belt" and "Kirkland greenstone belt", respectively. The green rectangle in the western part of A is an approximate outline of the subarea of Figures 9 and 10 (red block, Figure 8) (UTM NAD83, Zn17).

hosting gold deposits. Identically, the ranks also measure relative significance for gold deposit occurrence. The only difference between the ranks and the scores is their distribution, that is, the ranks are always evenly distributed (normalized to range from 0 to 1) but the distribution of the scores fluctuates vastly from case to case. The distributions are

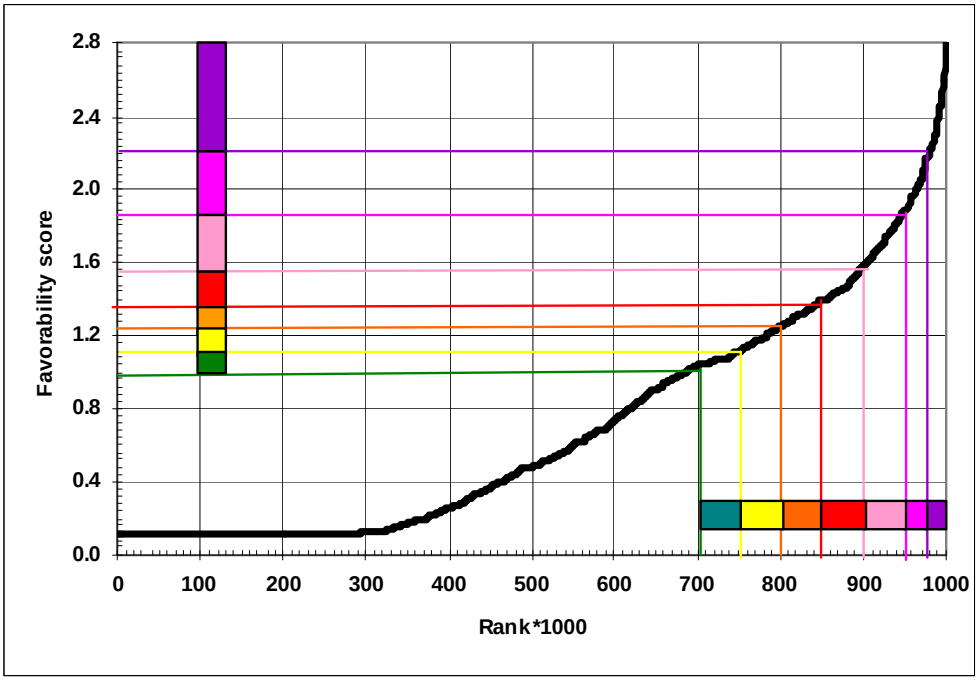

Figure 15: Sum scores related to the normalized rank described in the text for the gold potential map (Figure 14) in the Timmins-Kirkland study area, using the four decay functions illustrated in Figure 12(B). Dividing the scores or the ranks, the potential map containing the scores can be displayed. The colours in the colour bars are the same as in the map illustrating score-based potential in Figure 14.

dependent on how the decay functions have been established. The principal reason for using the ranks instead of the favourability scores is the even distribution of the ranks and therefore it is easier to divide them into the evenly distributed sizes. This is illustrated in Figure 15.

To illustrate how to obtain a rank of a favourability score, consider the Timmins-Kirkland study area. From the summed scores using the four weighted decay functions in Figure 12(B), 114,537,684 scores (one at each pixel) were computed for the 114,537,684 pixels in the study area. We sort the 114,537,684 scores in decreasing order. Then the ***rank*** of the pixel with the smallest score is 1 and the rank of the pixel with the largest score is 114,537,684. The ***normalized rank*** of a pixel is obtained by dividing the rank of the pixel by the total number of pixels in study area, 114,537,684. The normalized ranks range from 0.00000000873 (=1/114,537,684) to 1. The normalized ranks of the pixels are used to assign the pixels to the

"***potential***" classes. For convenience, the normalized ranks are simply referred to as "ranks" and the process is referred to as "ranking procedure."

Figure 15 shows the XY-plot of the sum scores and the rank for the gold potential map in Timmins-Kirkland study area using the four decay functions illustrated in Figure 12(B). Dividing the scores or the ranks, the potential map containing the sum scores can be displayed. An advantage of the use of the ranks is that they are easily interpretable and comparable between study areas. Consider a pixel with rank 0.998 in the Timmins-Kirkland study area as an example. There are only 2% (=1-0.998) of the 114,537,684 pixels (i.e., 229,075 pixels) that have higher scores than that of the pixel. Suppose that we wish to select an area consisting of about 5% of the study area for further exploration, then we may select all pixels with the ranks higher than 0.95. Alternatively, if we suppose that there is sufficient funding to explore the areas with the most potential comprising 100 km^2 (250,000 pixels with the size 20m x 20m) in the study area, then all the pixels with rank higher than 0.99782 (=1-250,000/114,537,684) are to be selected as the future exploration target.

Figure 14 (potential map) was constructed assigning the potential classes by slicing the ranks. The "Top 2.5%" class, the class most likely to contain gold deposits, consists of the pixels with the ranks higher than 0.975. The top ranked pixels are assigned a purple colour, shown in Figure

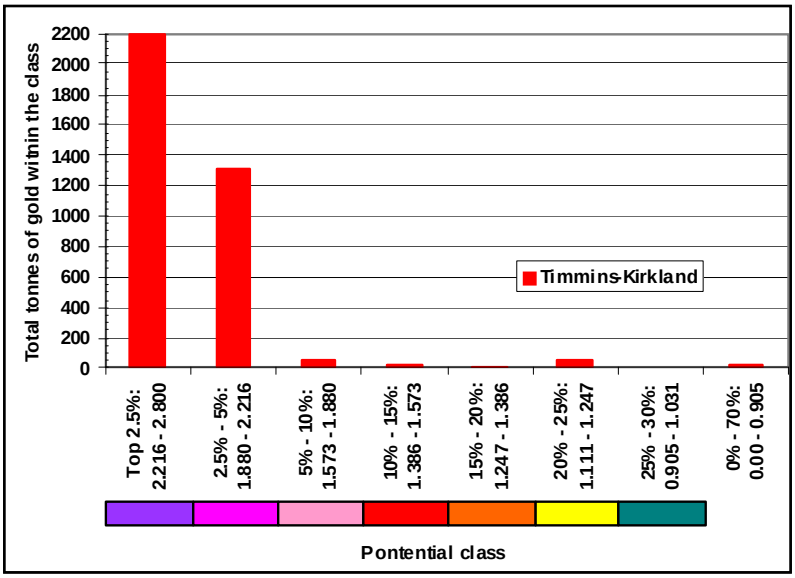

Figure 16: Tonnes of gold in each of the top seven potential classes in Figure 14. Seven colour bars in X-axis are same as the colours of the top seven classes in Figure 11. When we compare the top two classes (purple and magenta) with 39 discovered deposits, the purple and magenta classes contain 2,198 tonnes (70,667,341 ounces of gold; 60.3% of total gold) and 1,326 tonnes (42,213,930 ounces; 36% of total gold), respectively and these two classes include all five largest deposits shown as "a", "b", "c", "d" and "e" in Figure 14. The colour bar of the classes matches the colours in Figure 11.

14. The next highest potential class, "95-97.5%", contains the pixels with the ranks between

0.95 and 0.975 and magenta colour was assigned. Nine additional classes, "90-95%", "85-90%", "80-85%", "75-80%", "70-75%", "65-70%", "50-65%", "25-50%" and "0-25%" were obtained similar procedure. Each of two classes with the highest potential ("Top 2.5%" and "95-97.5 %") occupies 1,145 km^2 of the 45,815 km^2 in the study area. Equially, we can obtain the same results by slicing the corresponding average scores instead. If we select all pixels whose scores are higher than 2.216, it is identical to the earlier "Top 2.5% class". In the colour legend in Figure 14, the slicing values for both the ranges of the scores and the ranks were displayed for each potential class.

When we compared Figure 14 with the known 39 deposits containing 3,643 tonnes of gold, we obtained the graph in Figure 16. The purple and magenta classes contain 2,198 tonnes (70,667,341 ounces of gold; 60.3% of total gold) and 1,313 tonnes (42,213,930 ounces; 36% of total gold), respectively. All five largest deposits shown as "a", "b", "c", "d" and "e" in Figure 14 are included within these two classes. In the "Timmins greenstone belt" enclosed by the black ellipse **A** in Figure 14, these two classes occupy 827 km^2 and they contains 2,198 tonnes of gold among the discovered 39 deposits. The two classes within the "Kirkland greenstone belt" enclosed by the black ellipse **B** in Figure 14, however, occupy 889 km^2 and 1,326 tonnes of discovered deposits are contained in the two classes. On average, purple and magenta classes within the Timmins and Kirkland greenstone belts contain 2.641 (=2,198/827) and 1.491 (=1,326/889) tonnes per 1 km^2, respectively.

D) Gold potential map of Val D'Or greenstone belt using the same procedure

As used in the Timmins-Kirkland study area, the same four criteria, using the same decay functions, were used to generate a potential map (Figure 17(B)) for the Val D'Or district, another highly prolific gold producing region. Each of the four data layers was generated by computing the shortest distances from "Timiskaming-like" sediments, permissive faults, intrusions and ultramafic rocks at each pixel location.

As for Figure 14, each weighted and decayed function in Figure 12(B) provides a "***favourability score***" at each pixel for the corresponding criterion. To compare the potential in the Val D'Or area (Figure 17) with the potential for the Timmins-Kirkland area (Figure 14), the same ranges of the scores were used for both maps. Figure 18 shows the comparison of scores for the known resources in Val D'Or (blue bars) with Timmins-Kirkland Lake (red bars). Two classes with the most potential (represented on the map by the purple and magenta areas) contain 217 tonnes (6,976,712 ounces of gold; 22.7% of total gold) and 662 tonnes (21,283,794 ounces; 69.1% of total gold), respectively. Unexpectedly, the class with the highest potential (purple class) contains less gold in the Val D'Or area, in contrast with the Timmins-Kirkland study area (Figure 15), which contains 60.3% and 36.0% respectively for the same rank intervals However,

the two classes together contain 96.3% and 91.8% of all discovered deposits for Timmins-

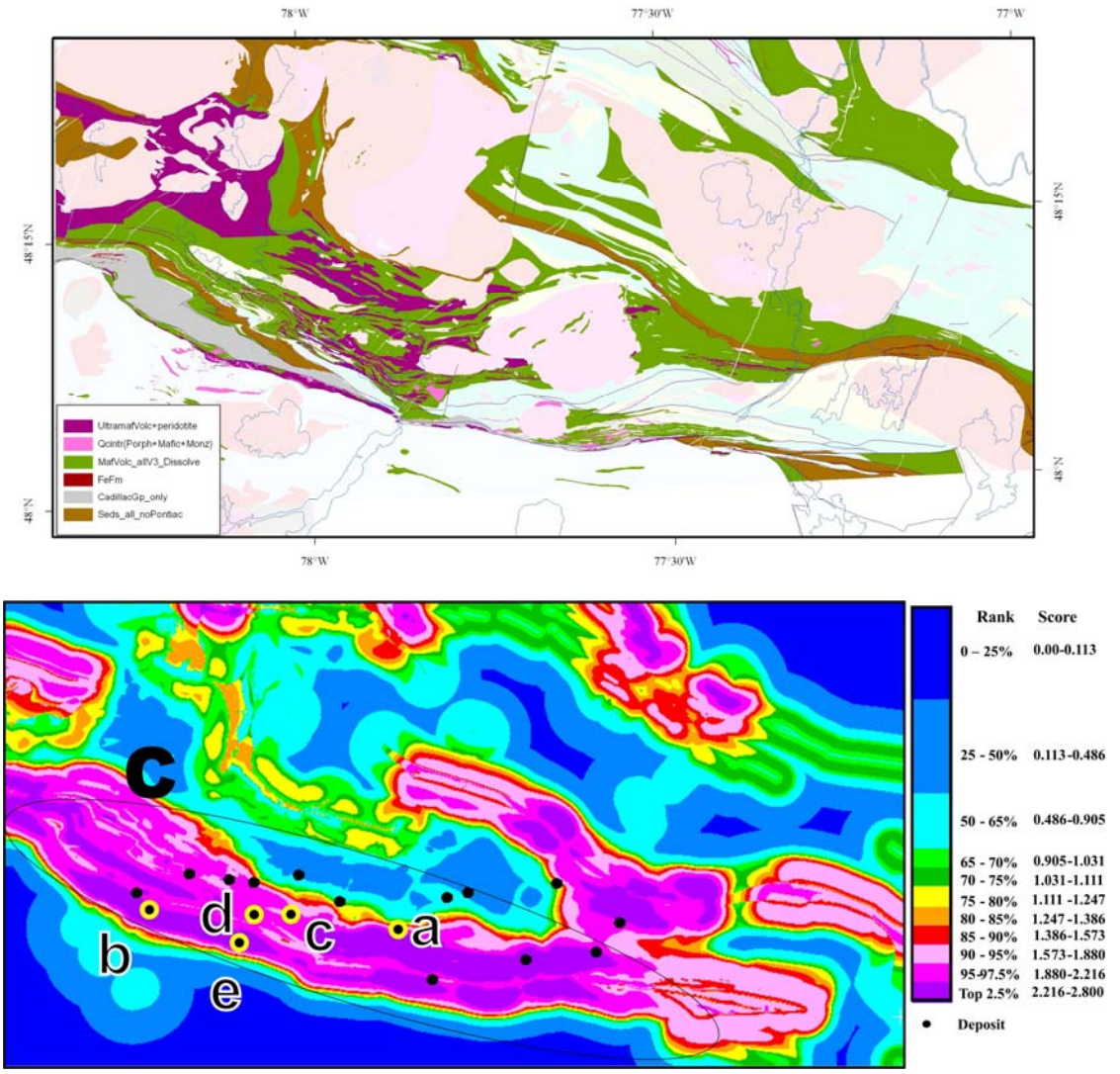

Figure 17: (A) Detailed geological map of Val-d'Or after Lamothe et al., 2005. (B) Gold potential map in Val d'Or study area. 18 black dots indicate the gold deposits containing, at least, 32,151 oz (1 tonne) of gold. Among the 18 deposits, the largest five deposits with 444 (a), 160(b), 98(c), 60(d) and 53(e) tonnes of gold are all located within top two potential classes (purple and magenta classes). The area enclosed by a black ellipse, **C** approximately represents the "Val d'Or greenstone belt".

Kirkland and Val d'Or areas and also include all five of the largest deposits ("a", "b", "c", "d" and "e" in Figures 14 and 17, respectively). Perhaps the upper two classes should be combined into one (upper 5%) class. Also, our analysis does not include the most recent developments in the district, including a large tonnage deposit by Osisko Mining Ltd. containing 245.8mt at 1.13 g/t: (http://www.osisko.com/pdfs/2010-03-22_Updated_reserve_and_resource_estimates.pdf.). In the "Val d'Or greenstone belt" (enclosed by the black ellipse C in Figure 17) these two classes occupy 592 km^2 and they contain 860 tonnes of gold among the discovered 18 deposits. On

average, the upper two (purple and magenta) classes within Val d'Or greenstone belt contains 1.453 (=860/592) tonnes of gold per 1 km^2. This compares with 2.641 and 1.491 tonnes per 1 km^2 for Timmins and Kirkland greenstone belts, respectively (Figure 18).

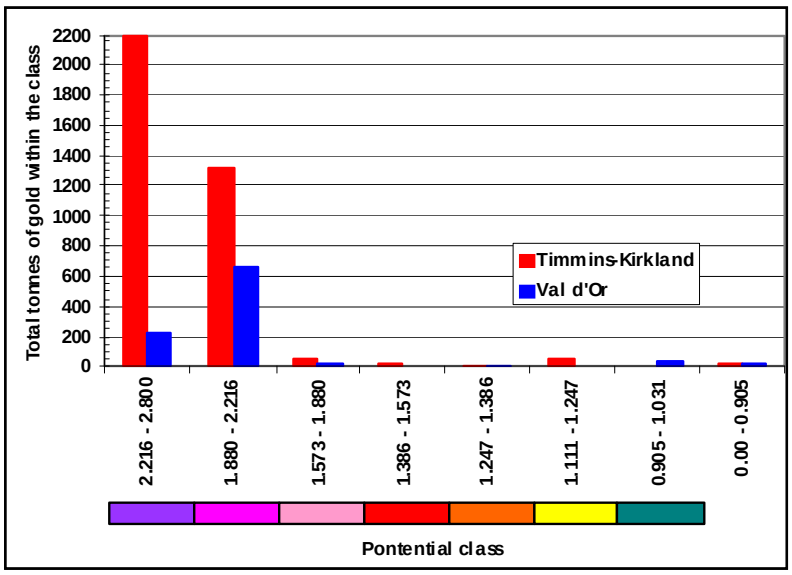

Figure 18: Tonnes of gold in each of the top seven potential classes in Figures 14 and 17. Seven colour bars on X-axis are same as the colours of the top seven classes in Figures 14 and 17. Top two classes (purple and magenta) in Figures 14 and 17 occupy 2,291km and 776km^2 and contain 109,119,632 ounces and 27,456,737 ounces of gold (93.2% of total gold of 117,125,168 ounces) and 89.1% of total gold of 30,800,415 ounces), respectively.

Summary of the results for the Eastern Abitibi analysis:

Using the four criteria that are almost universally available on geological compilation maps, the method successfully 'found' the majority of the gold deposits. Numerous additional areas of relatively high potential are also identified (Figure 14), particularly to the southwest of the Kirkland Lake (Matachewan area) and Timmins (Swayze district). Both of these areas contain gold deposits, which although economically productive, have not been historically the "super-giant' producers present in Timmins and Kirkland Lake. In order to provide better discrimination of potential, it would be ideal if additional criteria could be used.

Improvements in the methodology could be attained once better validation of the genetic implications of each criterion is determined, and data for the additional criteria outlined in Table 1 are embedded in the compilation maps. The maps used (Ayer et al., 2004) and (Lamothe et al.,

2005) were easily adapted for use in the GIS-based approach used herein. Consistent and simple legends that clearly identify the key criteria as mapped units were key.

Using the Slave Province Compilation to Test Procedure for Individual Greenstone Belts

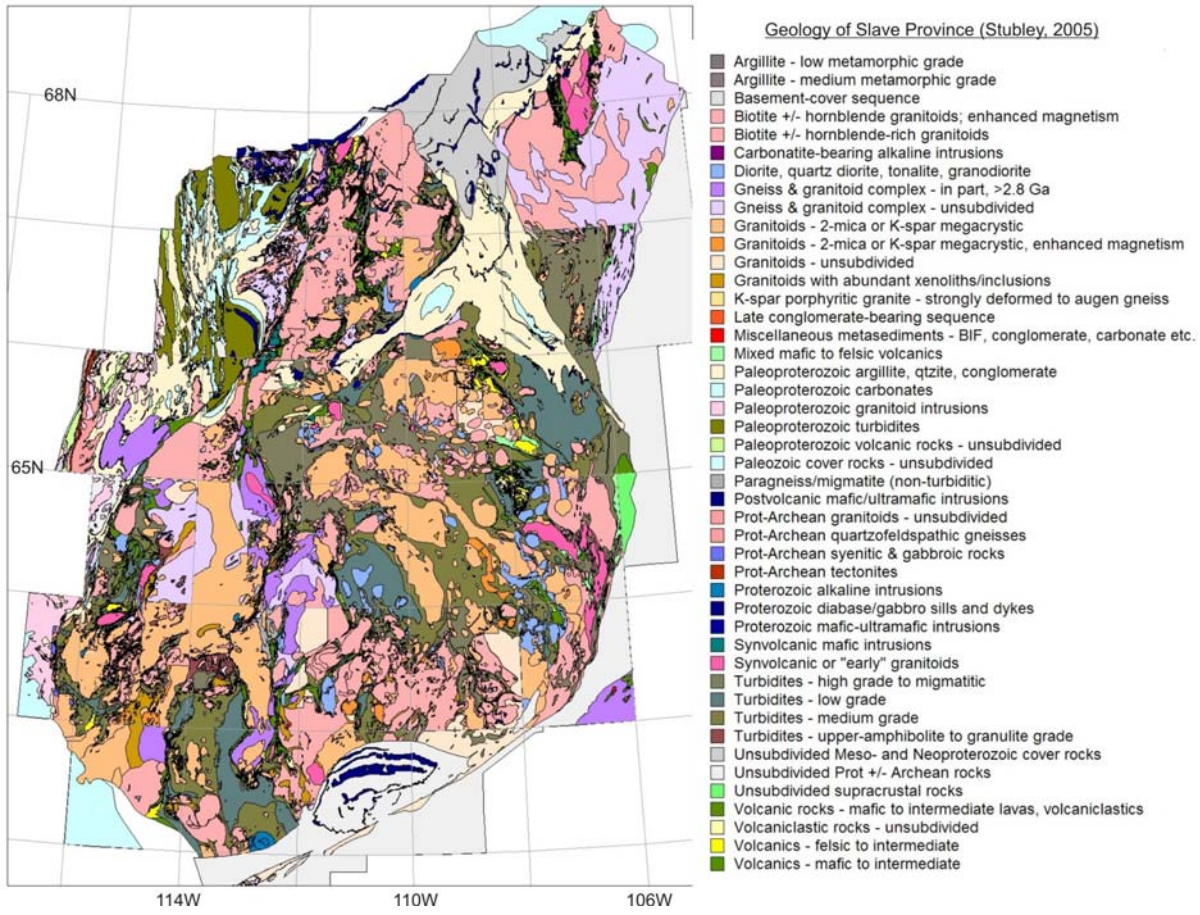

Figure 19: Geology of Slave Province, after Stubley, 2005. Legend simplified from codes provided in the digital data set.

As part of our mandate to assist the GSC with its program planning in the northern parts of Canada, we undertook to assess the entire Slave Province for its gold potential, using a recent geological compilation (Stubley, 2005). This map was also used for the previous study (VMS deposits) and was compiled from a variety of source maps of highly variable quality and scale. The Slave Province contains 18 greenstone belts (Figures 19 and 20), several containing either past, present or near production gold deposits. Each of these was examined separately, based on the possibility that each has a specific but different structural trend relative to the others, and that the database underlying the compilation for each of these is highly variable in quality. Although all 18 greenstone belts in Slave Provinces contain permissive faults, only nine of these contain

“Archean conglomerate”. It is uncertain if this reflects a real absence of this key criterion, or if the database is not sufficiently complete, and did not include this unit. We will **individually assess the gold potential of the nine greenstone belts containing Archean** conglomerate (Figure 20). Later in this section, we will consider the effect of adding iron formation as a factor.

Each of the data layers was generated by computing the shortest distances from the presences of Archean conglomerate, permissive faults, granite-porphyry and ultramafic supracrustal rocks at each pixel location. The set of four decay functions (Figure 12B) was used to generate the

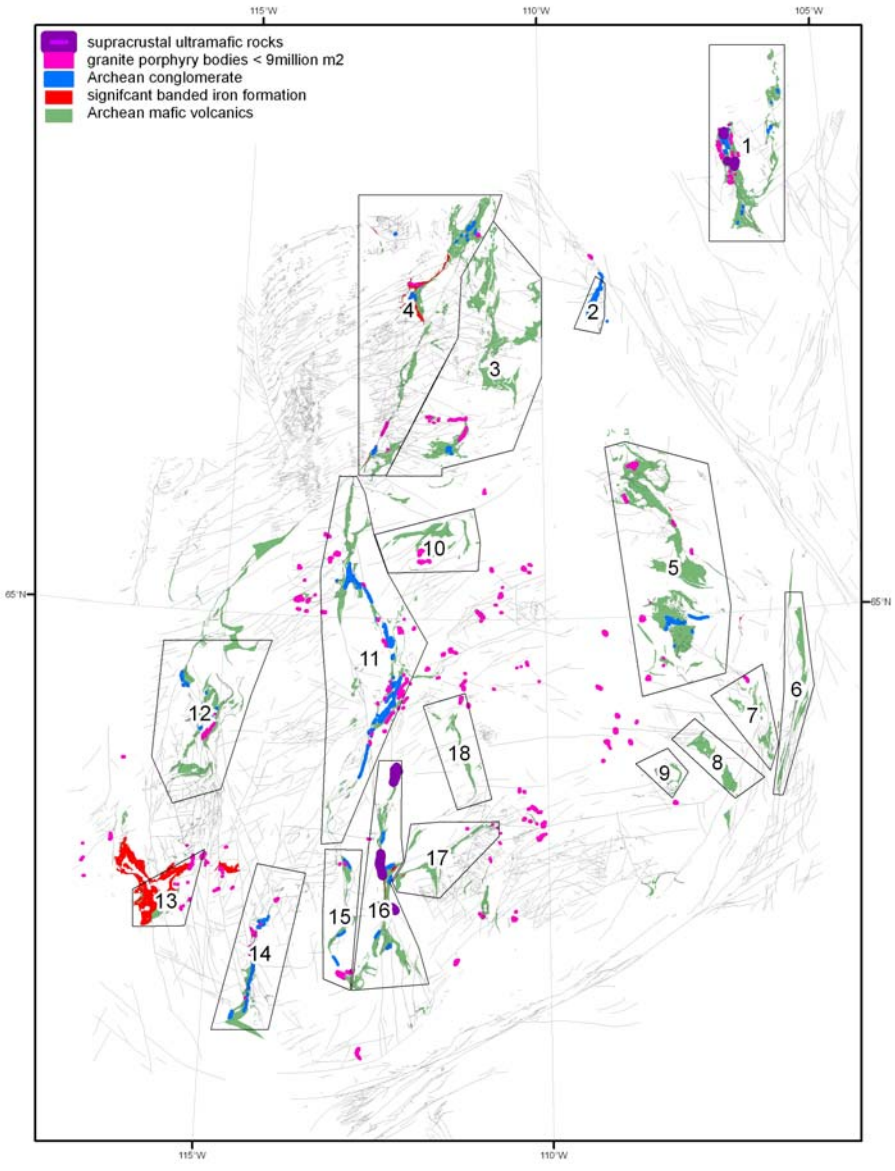

Figure 20: The four map units from the Stubley (2005) map used in making the potential maps for each greenstone belt: Archean conglomerate ("Timiskaming-like" sediments), granite-porphyry, ultramafic supracrustal rocks and permissive faults. Only areas 1, 3, 4, 5, 11, 12, 14, 15 and 16 could be evaluated (see text) as the remainder lacked sufficiently detailed geological information.

following potential maps.

A) Gold potential in Hope Bay greenstone belt: Belt #1

Study area # 1 (Figure 20: greenstone belt #1) is comprised of 2780 x 7300 pixels and each pixel occupies 20 x 20 m on ground. This area contains 3 near-production deposits.

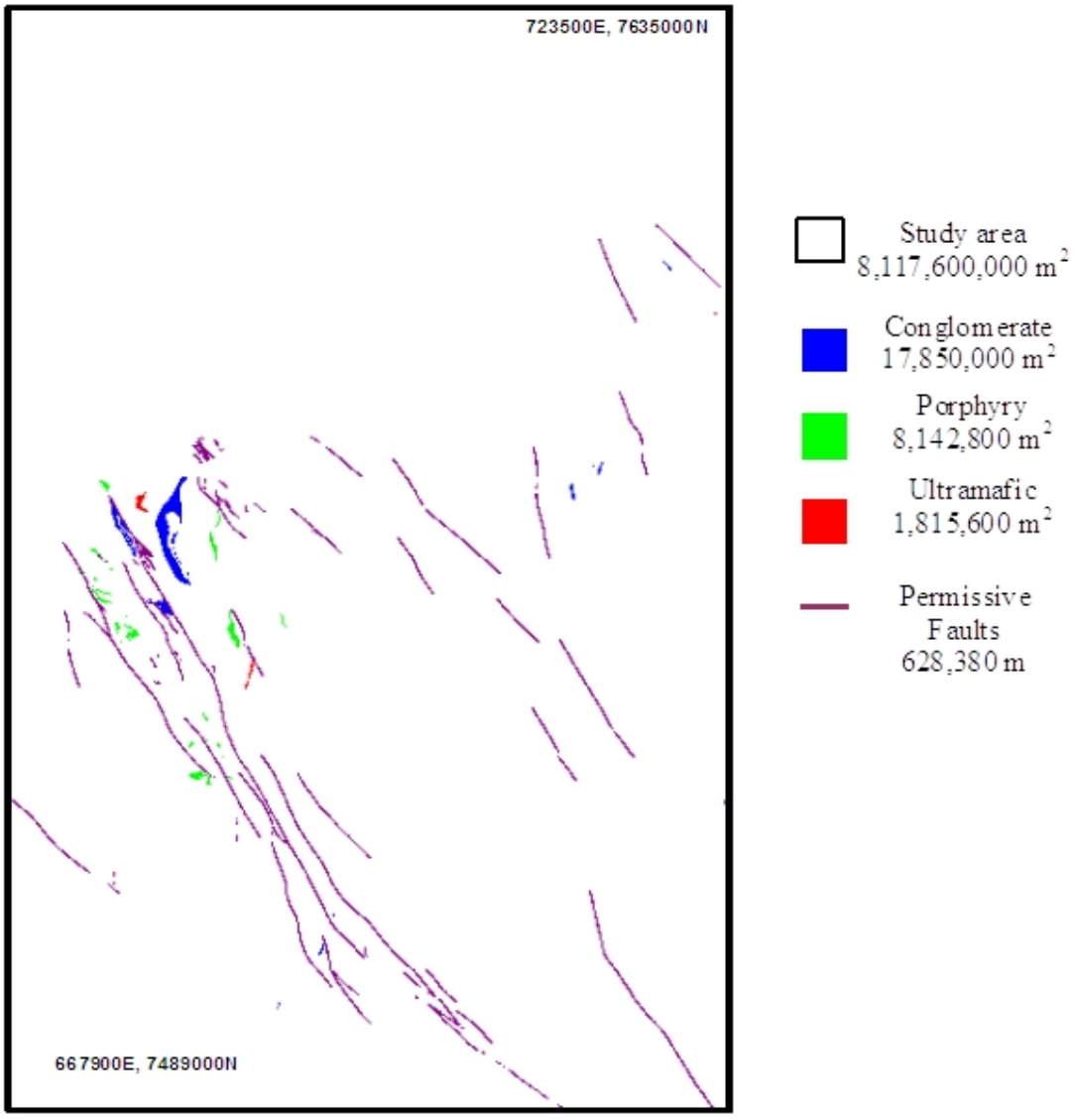

Figure 21: Permissive faults in the Hope bay area (using the same method as described for the Timmins area, above) and location of three geological units, Archean conglomerate ("Timiskaming-like" sediments), granite-porphyry, and ultramafic supracrustal rocks (UTM NAD83, Zn12).

This belt contains all four geological units, Archean conglomerate, granite-porphyry, ultramafic supracrustal rocks and permissive faults (Figure 21). Each of the four data layers was generated by computing the shortest distances from the presence of these four criteria at each pixel location. The same set of decay functions shown in Figure 12(B) was used to generate the following potential map for Hope Bay greenstone belt (Figure 22).

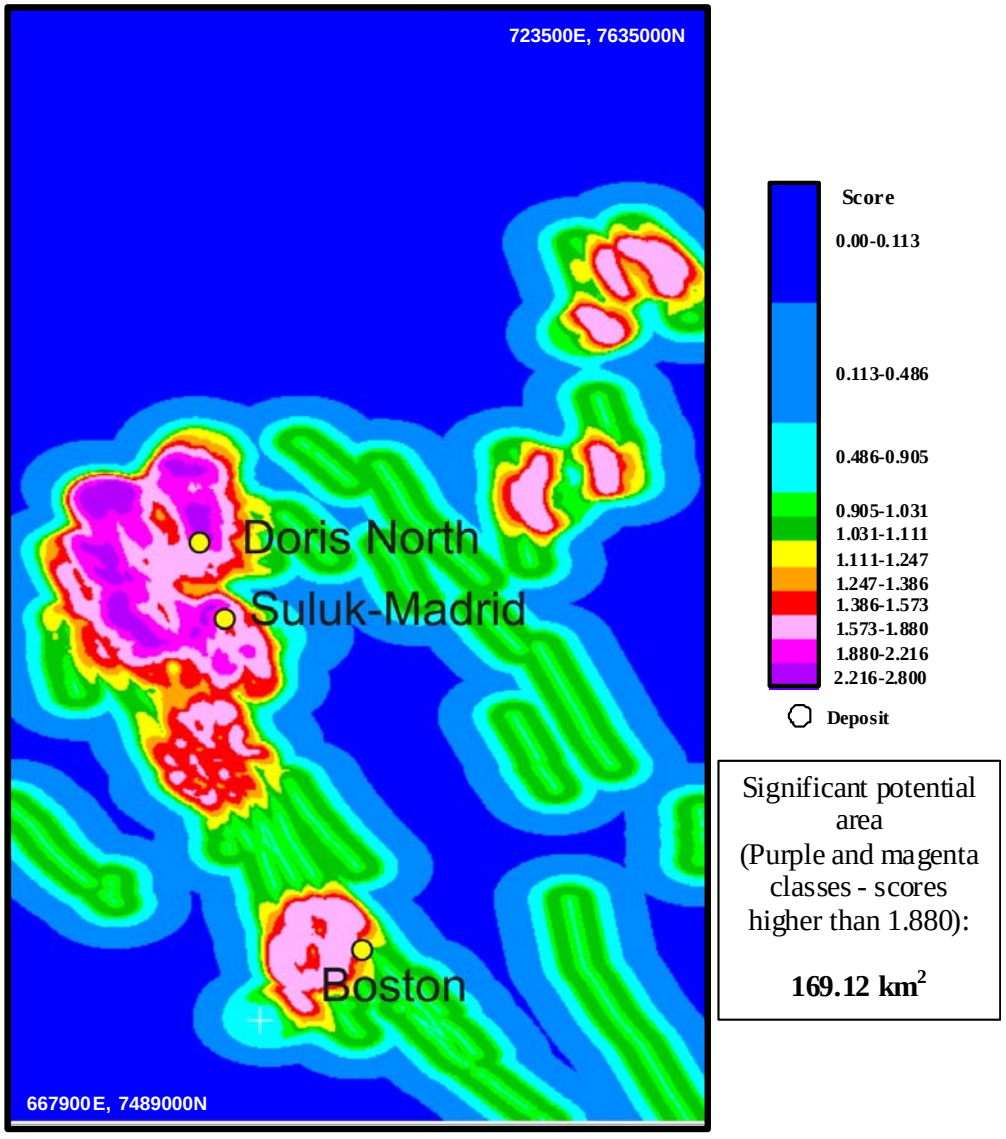

Figure 22: Gold potential map in Hope Bay greenstone belt using the distances from the permissive faults and three geological units: Note that the three near-production deposits are within the three highest ranked classes (UTM NAD83, Zn12).

B) Gold potential in greenstone belts #3 and 4

Study area: 6722 x 10430 pixels; each pixel occupies 20 x 20 m

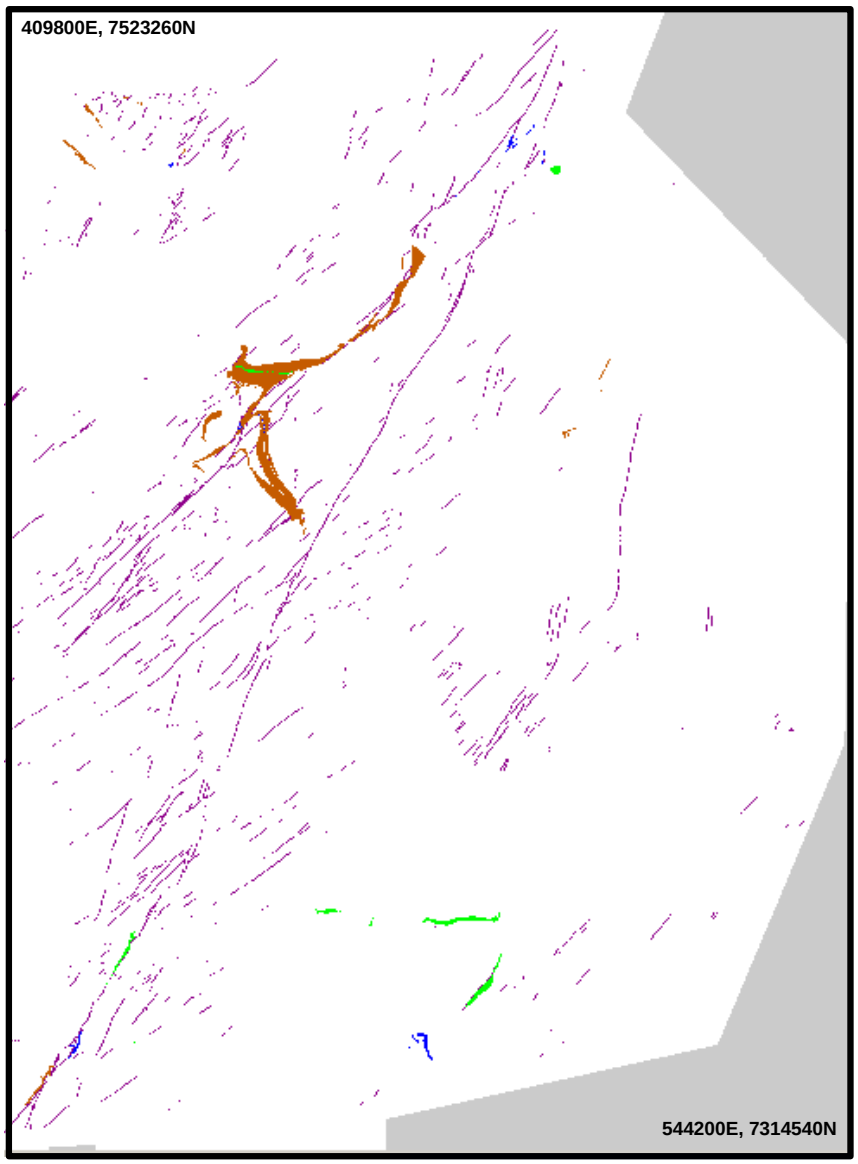

Study area
24,926,580,400 m^2

Conglomerate
9,534,800 m^2

Porphyry
24,877,200 m^2

Ultramafic
None

Iron formation
142,494,400 m^2

Permissive Faults
2,230,780 m

.Figure 23: Permissive faults and three geological units, Archean conglomerate ("Timiskaming-like" sediments), granite-porphyry, iron formation in belts 3 and 4 ((UTM NAD83, Zn12).

The three geological units considered are Archean conglomerate ("Timiskaming-like" sediments), granite-porphyry and permissive faults, as shown Figure 23. Each of the three data

layers was generated by computing the shortest distances from the presences of Archean conglomerate, permissive faults and granite-porphyry at each pixel location. The same four decay functions shown in Figure 12(B) were used to generate the potential map for greenstone belts #3 and 4 shown (Figure 24).

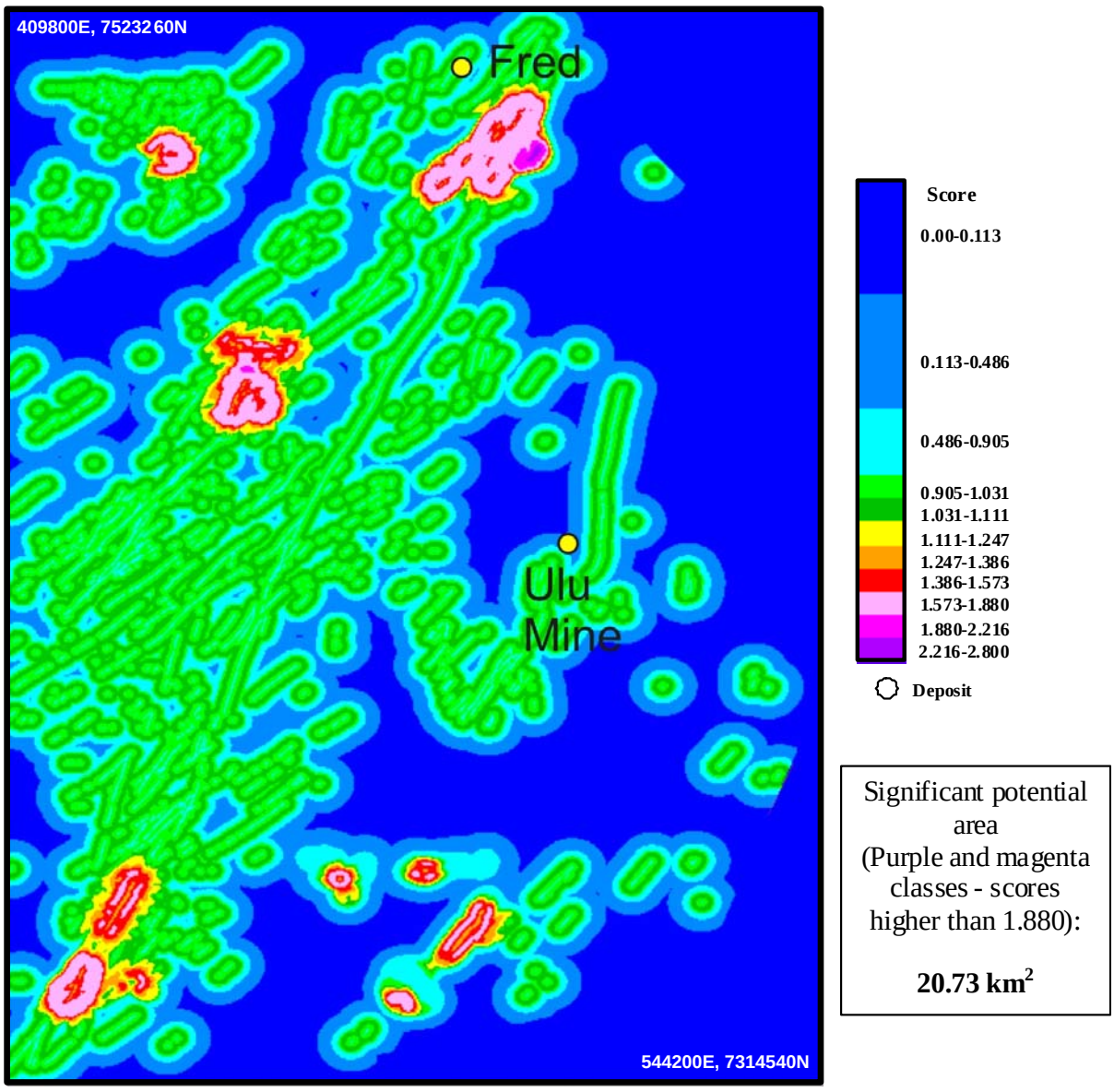

Figure 24: Gold potential map in greenstone belts #3 and 4 (UTM NAD83, Zn12).

C) Gold potential in greenstone belt #5: Hackett River belt

Study area: 4700 x 9500 pixels; each pixel occupies 20 x 20 m.

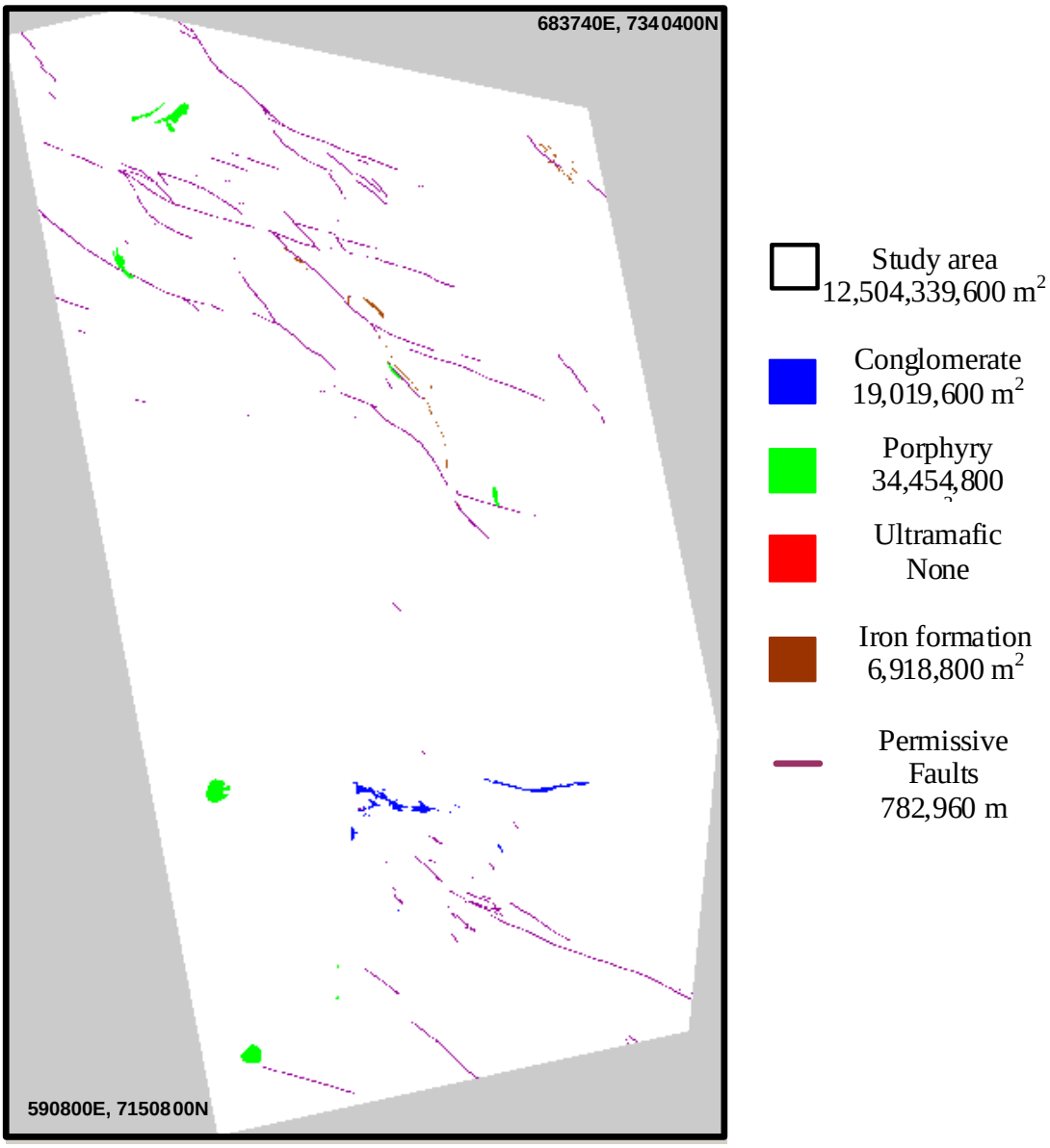

Figure 25: Hackett River area: Permissive faults and two geological units, Archean conglomerate ("Timiskaming-like" sediments) and granite-porphyry (UTM NAD83, Zn12).

The three geological units considered are Archean conglomerate ("Timiskaming-like" sediments), granite-porphyry and permissive faults, as are shown in Figure 25. Each of the three data layers was generated by computing the shortest distances from the presences of Archean conglomerate, permissive faults and granite-porphyry at each pixel location. The same set of decay functions shown in Figure 12(B) was used to generate the following potential map for greenstone belt shown in Figure 26.

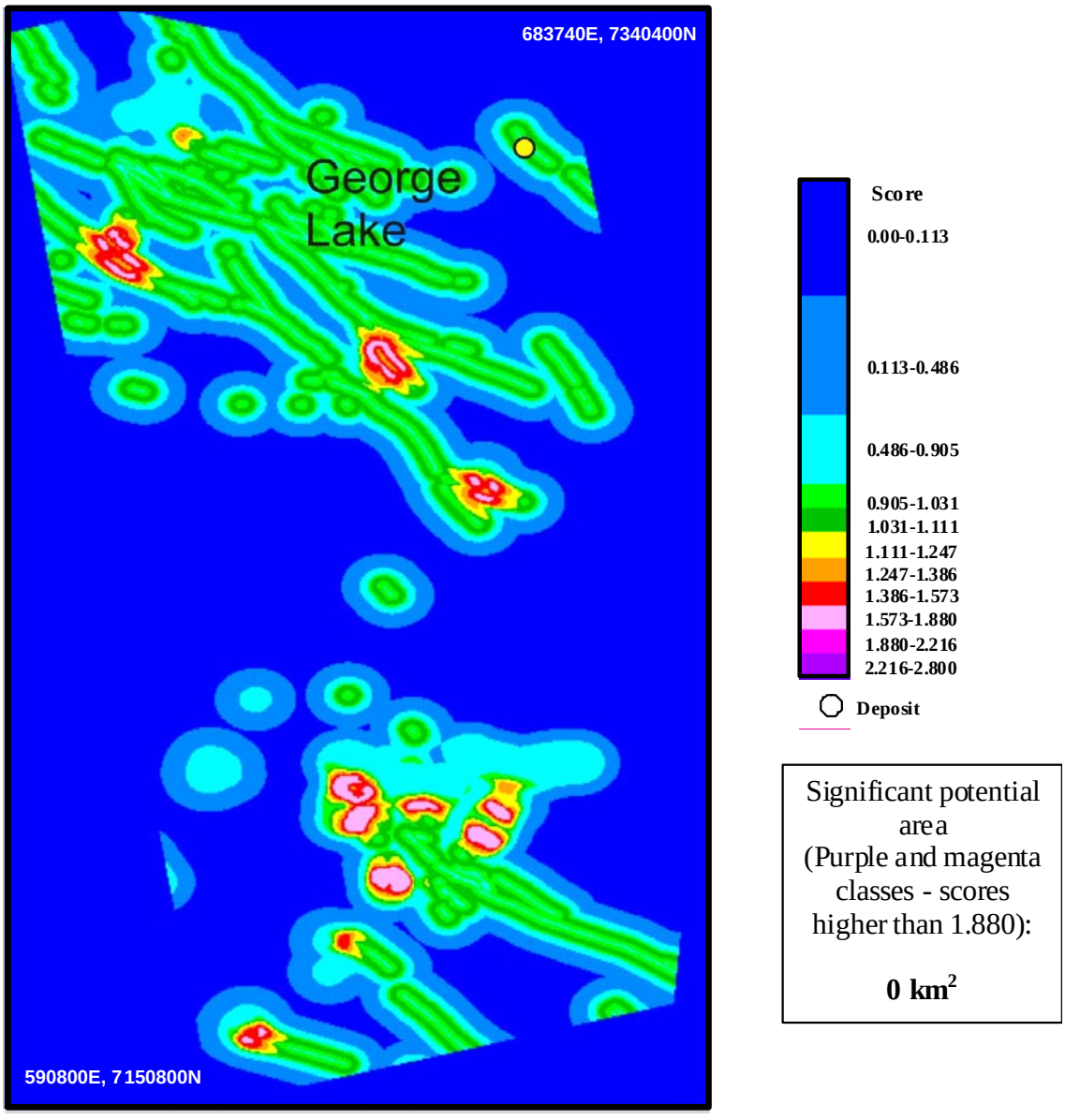

Figure 26: Gold potential map in greenstone belt #5 (Hackett River) (UTM NAD83, Zn12).

D) Gold potential in greenstone belt #11

Study area: 4000 x 13700 pixels; each pixel occupies 20 x 20m.

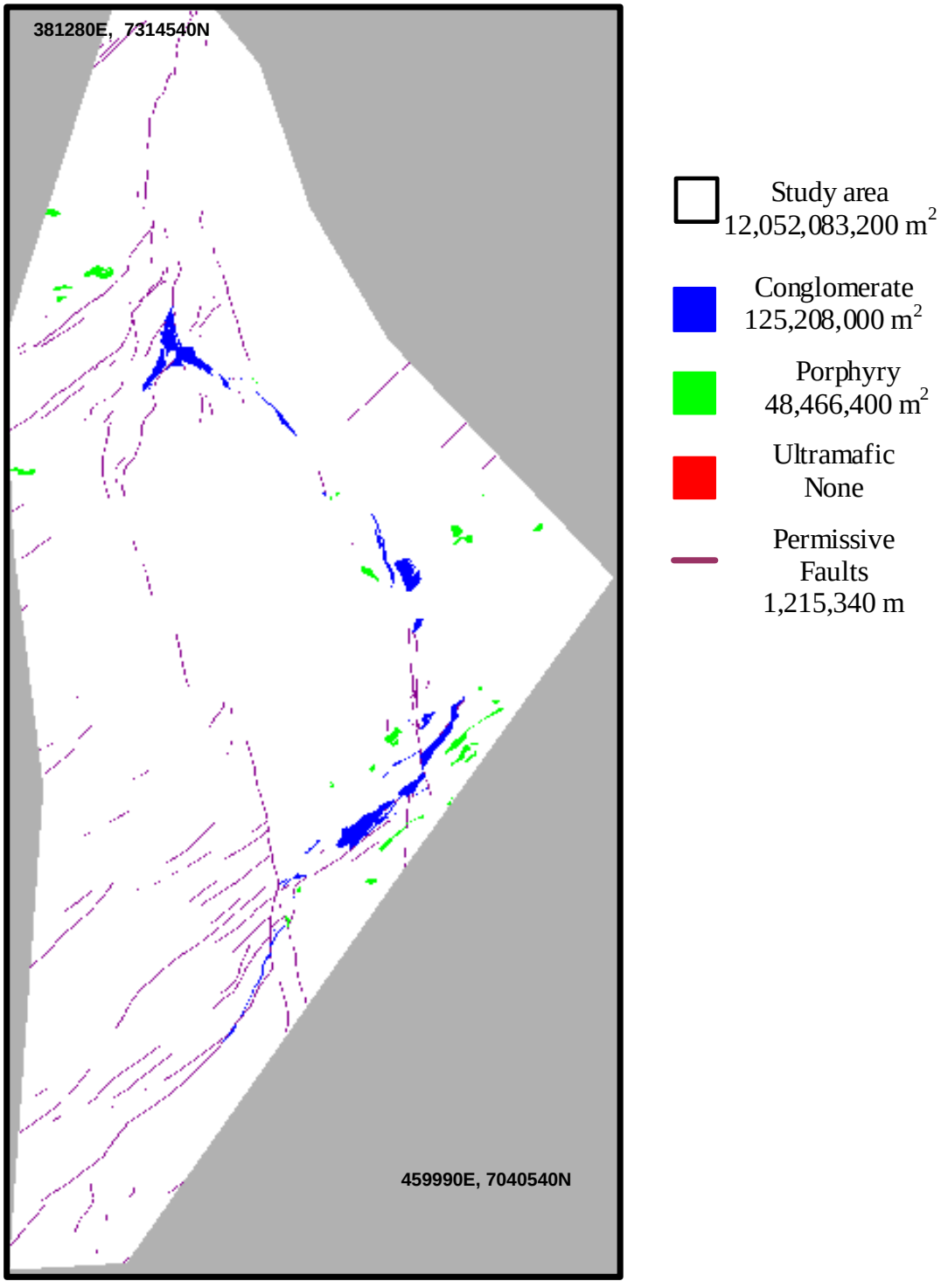

Figure 27: Belt #11: Permissive faults and two geological units, Archean conglomerate and granite-porphyry in greenstone belt #11 (UTM NAD83, Zn12).

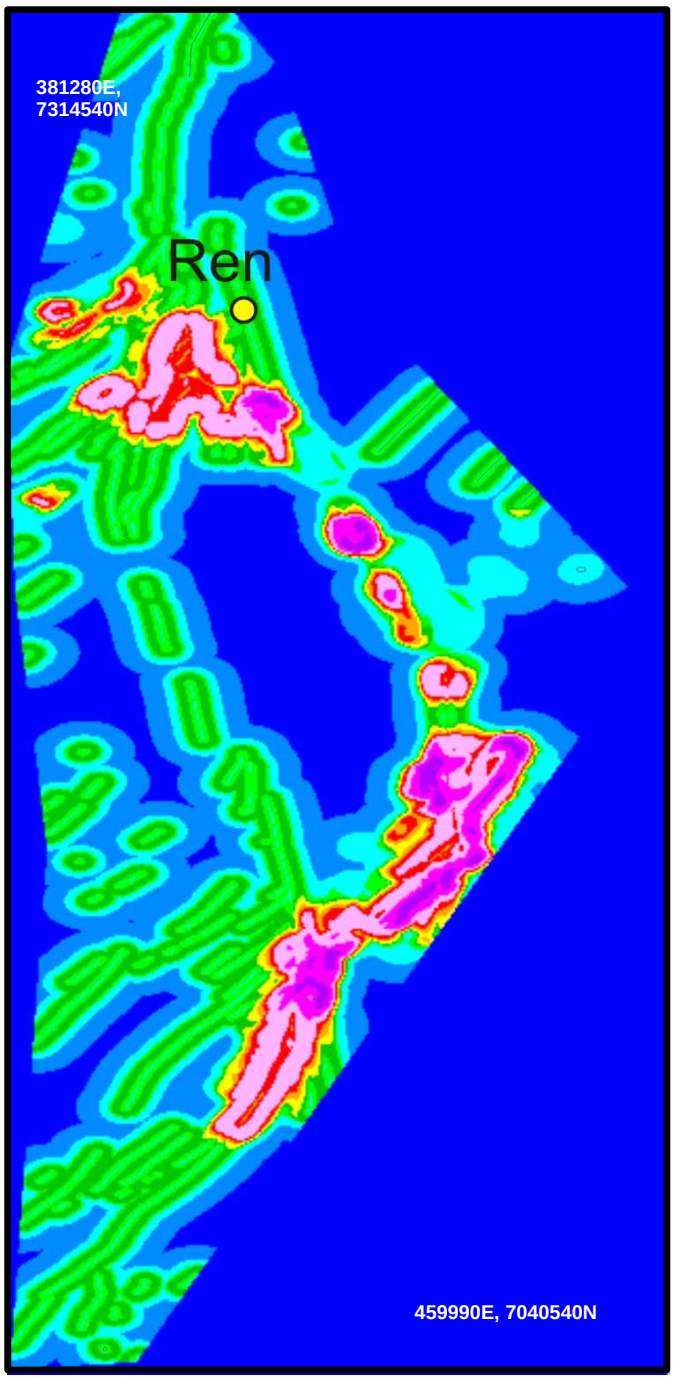

Figure 28: Gold potential map in greenstone belt #11 (UTM NAD83, Zn12).

The three geological units considered are Archean conglomerate ("Timiskaming-like" sediments), granite-porphyry and permissive faults, as are shown Figure 27. Each of the three data layers was generated by computing the shortest distances from the presences of Archean conglomerate, permissive faults and granite-porphyry at each pixel location. The same set of

decay functions shown in Figure 12(B) was used to generate the potential map for greenstone belt shown in Figure 28.

E) Gold potential in greenstone belt #12

Study area: 5000 x 6150 pixels; each pixel occupies 20 x20m.

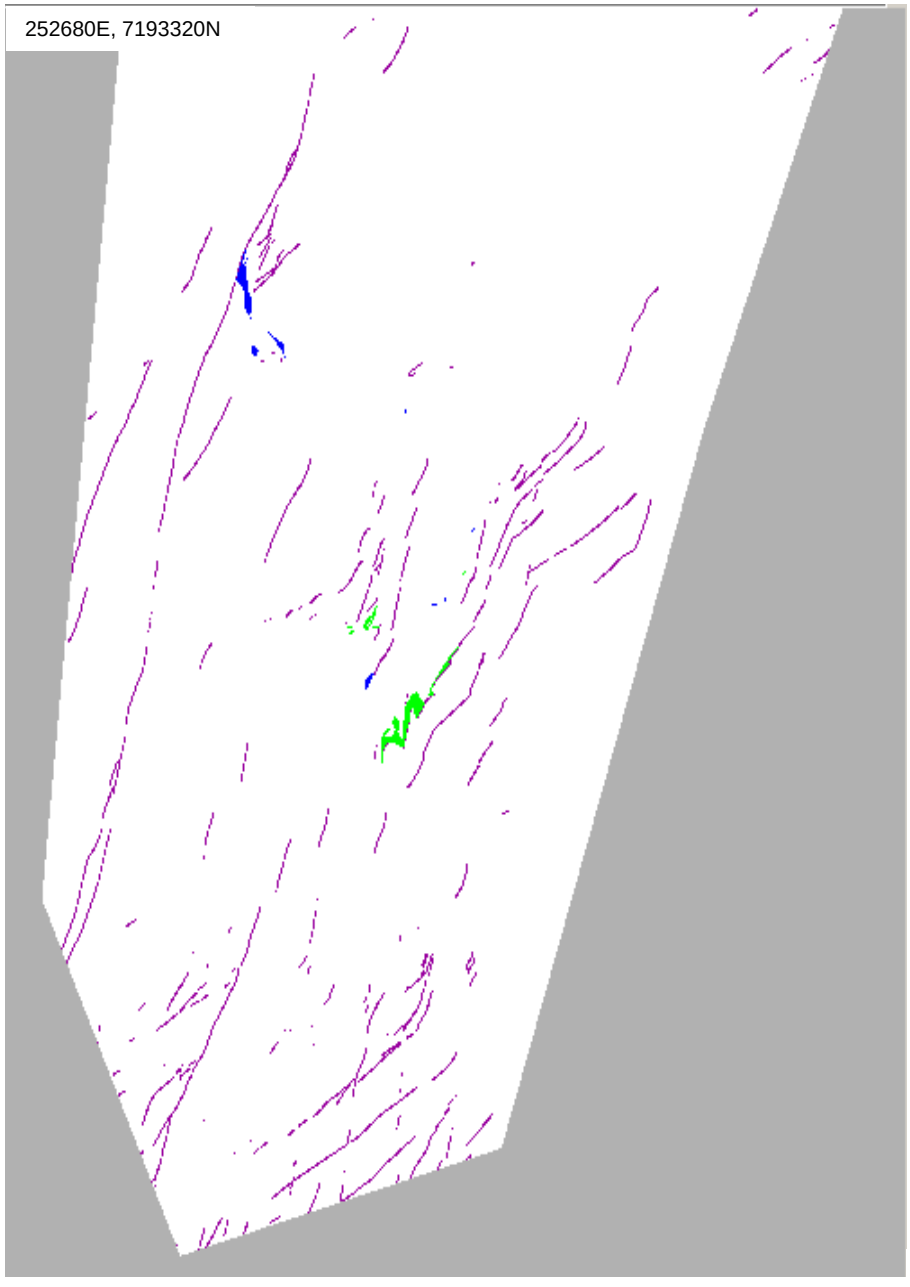

Figure 29: Permissive faults and three geological units, Archean conglomerate ("Timiskaming-like" sediments), granite-porphyry, and ultramafic supracrustal rocks in belt #12 (UTM NAD83, Zn12).

The three geological units considered are Archean conglomerate ("Timiskaming-like" sediments), granite-porphyry and permissive faults, as shown Figure 29. Each of the three data layers was generated by computing the shortest distances from the presences of conglomerate, Permissive faults and granite-porphyry at each pixel location. Three of the same four decay functions shown in Figure 12(B) were used to generate the following potential map for greenstone belt #12 shown in Figure 30.

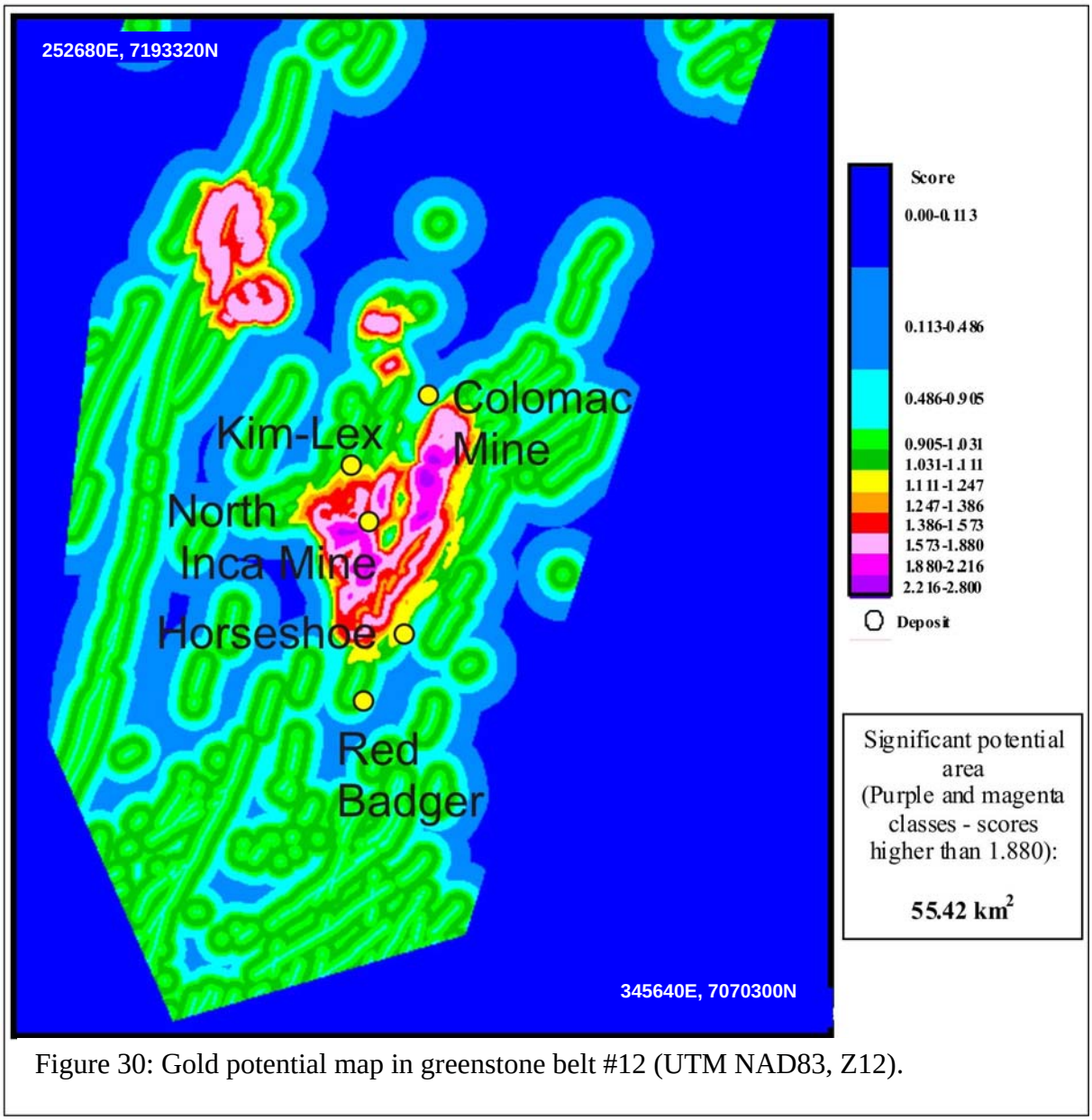

Figure 30: Gold potential map in greenstone belt #12 (UTM NAD83, Z12).

F) Gold potential in greenstone belt #14: Yellowknife

Study area: 4000 x 6315 pixels; each pixel occupies 20 x 20 m.

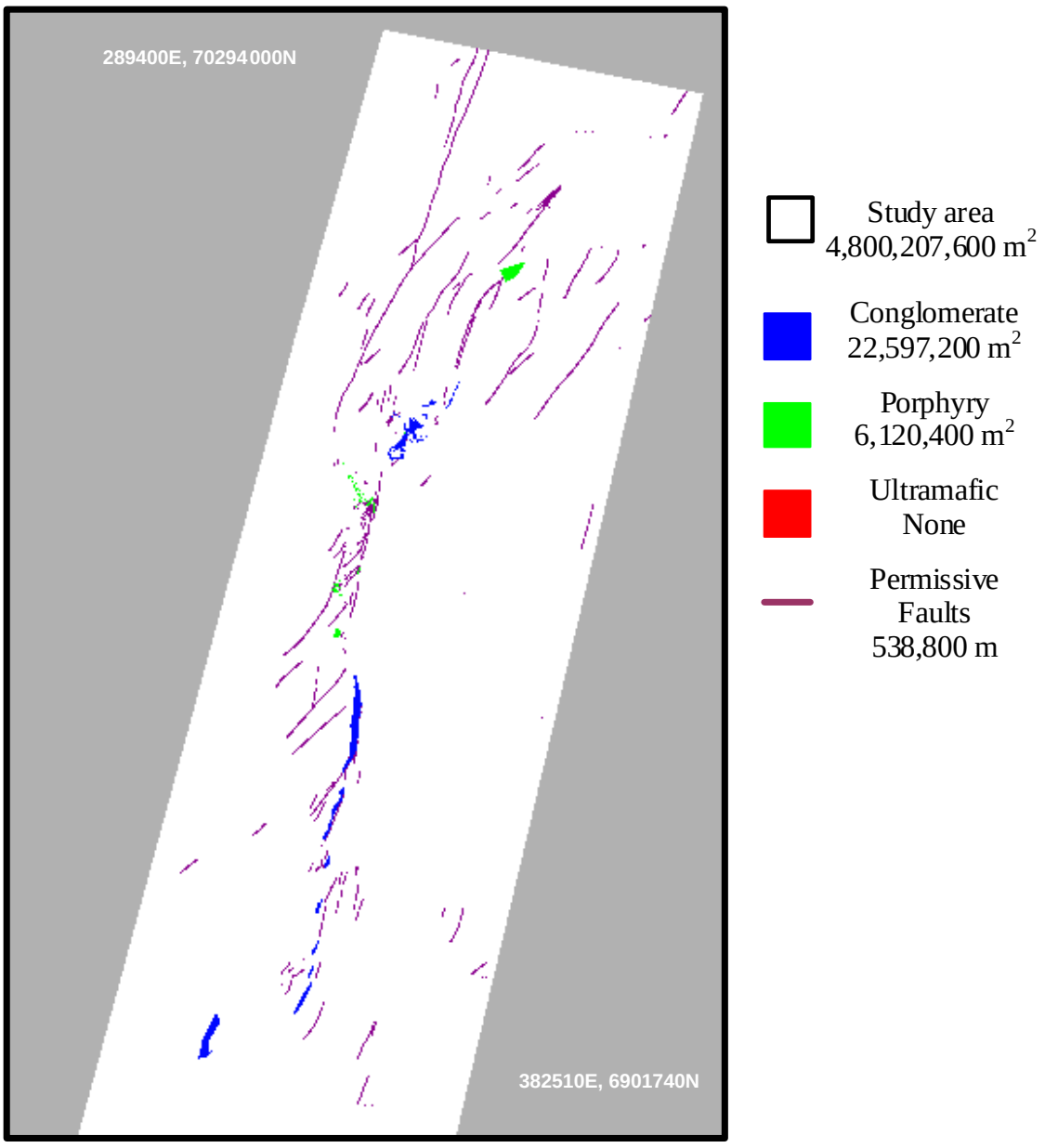

Figure 31: Permissive faults and two geological units, Archean conglomerate ("Timiskaming-like" sediments), granite-porphyry, Yellowknife greenstone belt (UTM NAD83, Zn12).

The three geological units considered are Archean conglomerate ("Timiskaming-like" sediments), granite-porphyry and permissive faults. The three data layers were generated by computing the shortest distances from the presence of conglomerate, permissive faults and granite-porphyry at each pixel location. Three of the same four decay functions in Figure 12(B) are used to generate the potential map for greenstone belt #14 (Yellowknife belt) (Figure 32).

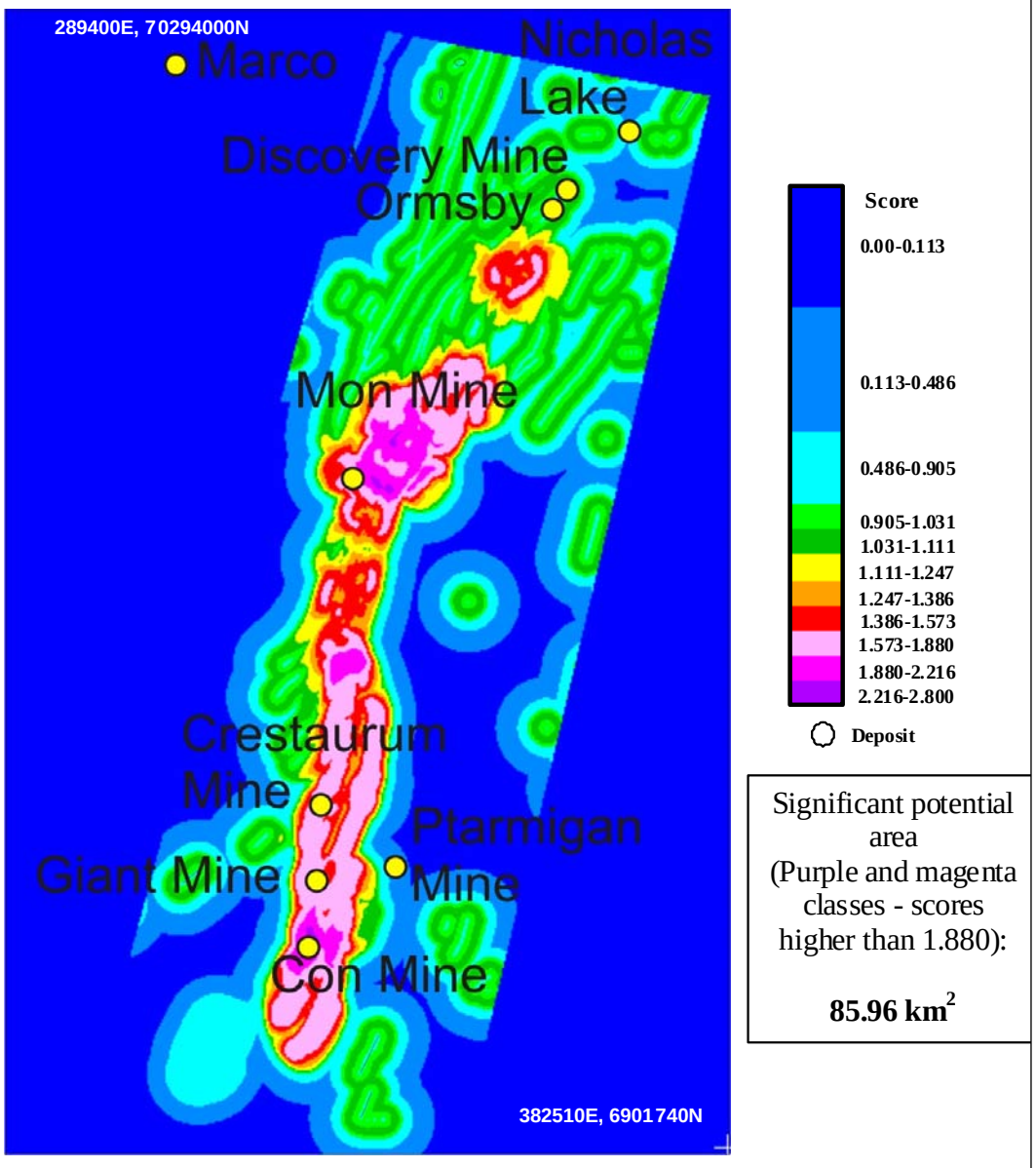

Figure 32: Gold potential map in Yellowknife greenstone belt (#14) using the distances from the permissive faults and two geological units: Archean conglomerate ("Timiskaming-like" sediments) and granite-porphyry (UTM NAD83, Zn12).

G) Gold potential in greenstone belt #15

Study area: 1600 x 5360 pixels; each pixel occupies 20 x 20 m.

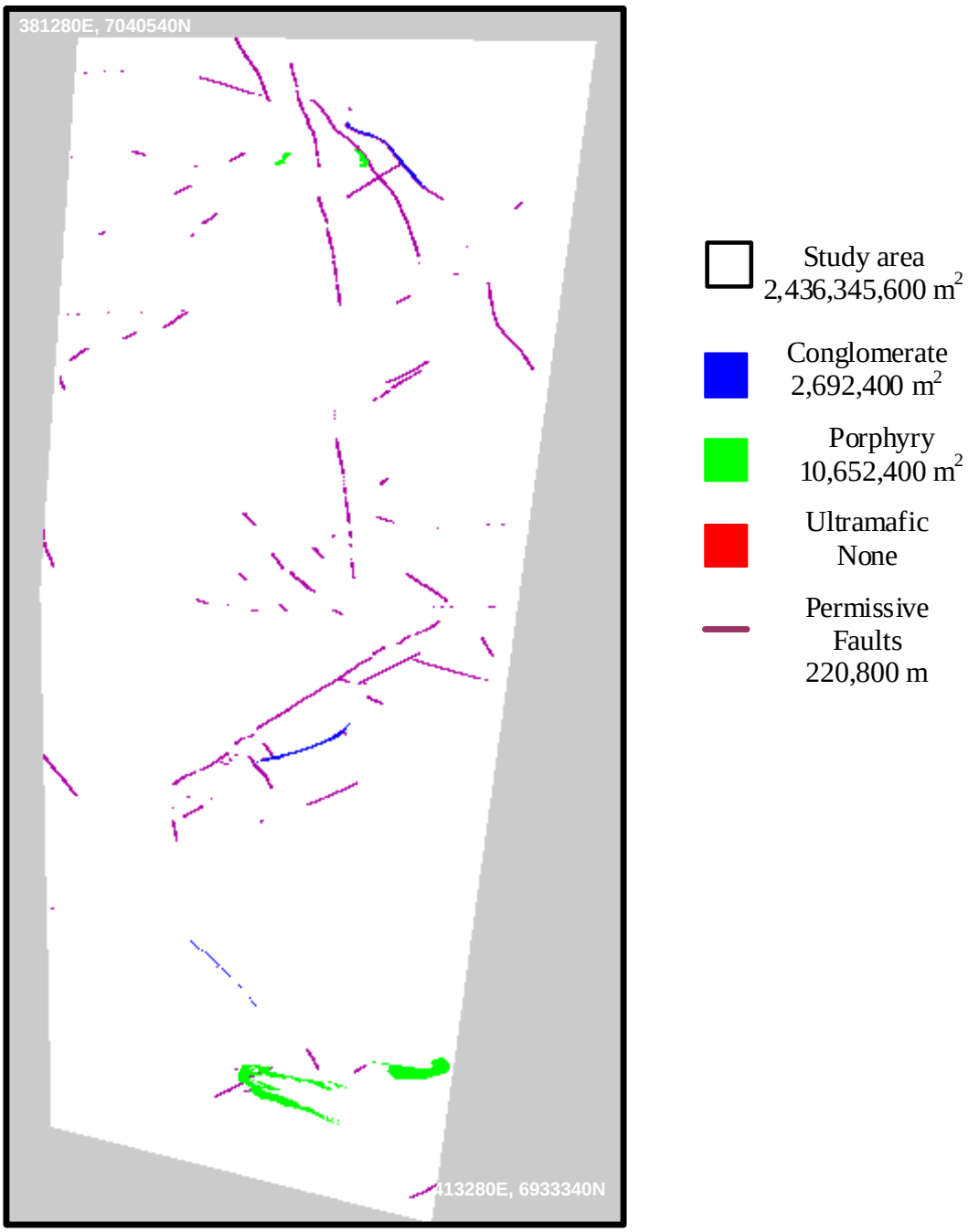

Figure 33 Permissive faults and three geological units, belt 15; Archean conglomerate ("Timiskaming-like" sediments), granite-porphyry, and ultramafic supracrustal rocks (UTM NAD83, Zn12).

This belt contains all four geological units, Archean conglomerate, granite-porphyry, ultramafic supracrustal rocks and permissive faults, as shown Figure 33. Each of the four data layers was generated by computing the shortest distances from the presence of these four key indicators at each pixel location. The same decay functions shown in Figure 12(B) were used to generate the following potential map this greenstone belt (Figure 34).

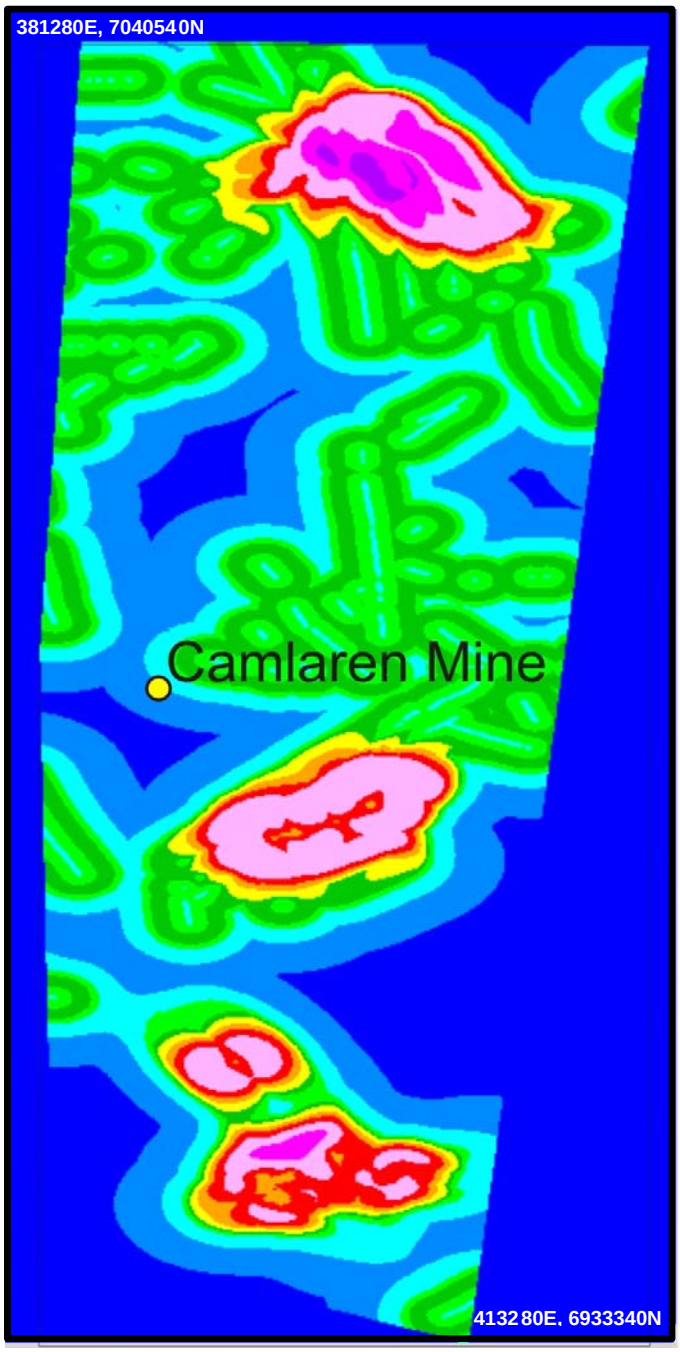

Figure 34: Gold potential map in greenstone belt #15 (UTM NAD83, Zn12).

H) Gold potential in greenstone belt #16

Study area: 3000 x 8560 pixels; each pixel occupies 20 x 20 m

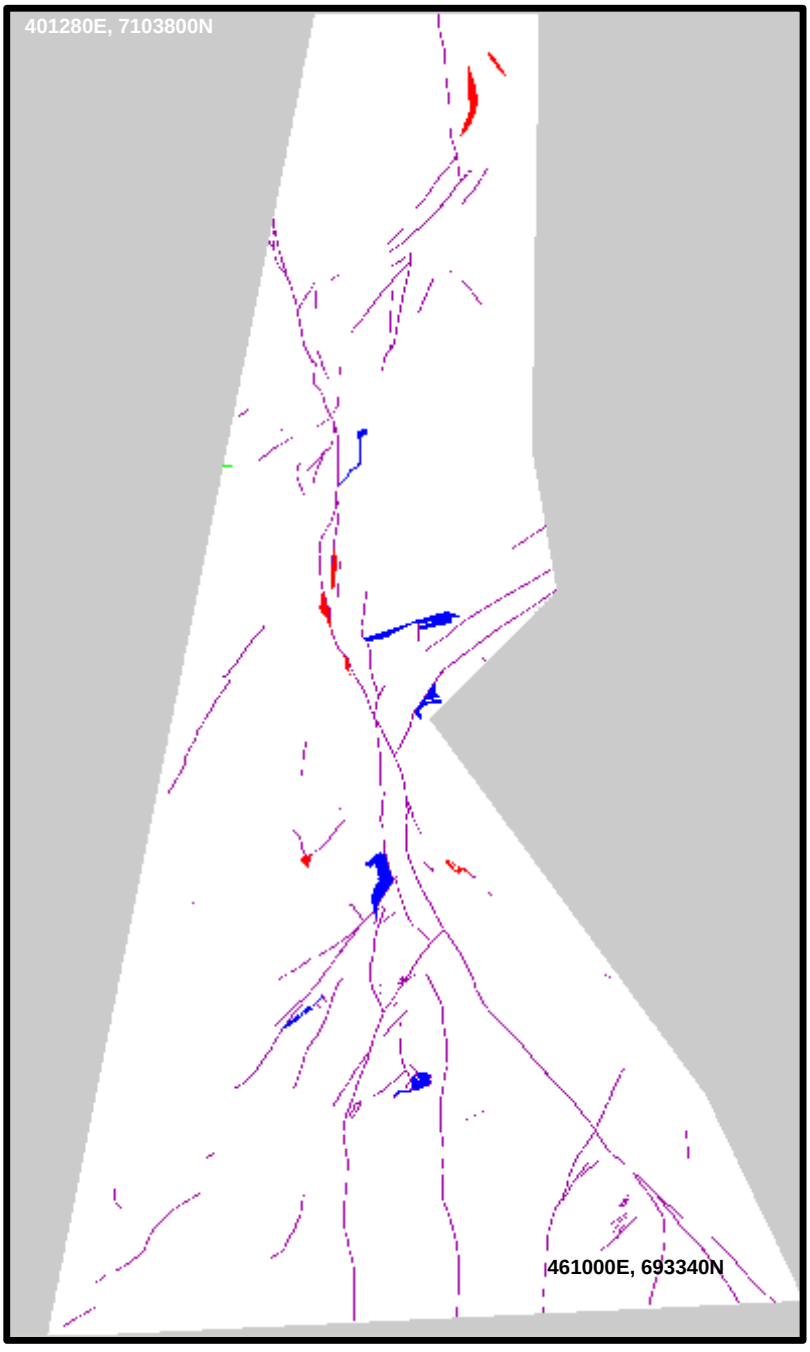

Figure 35: Permissive faults and three geological units, belt #16; Archean conglomerate ("Timiskaming-like" sediments), granite-porphyry, and ultramafic supracrustal rocks (UTM NAD83, Zn12).

For this belt, all four geological units, Archean conglomerate, granite-porphyry, ultramafic

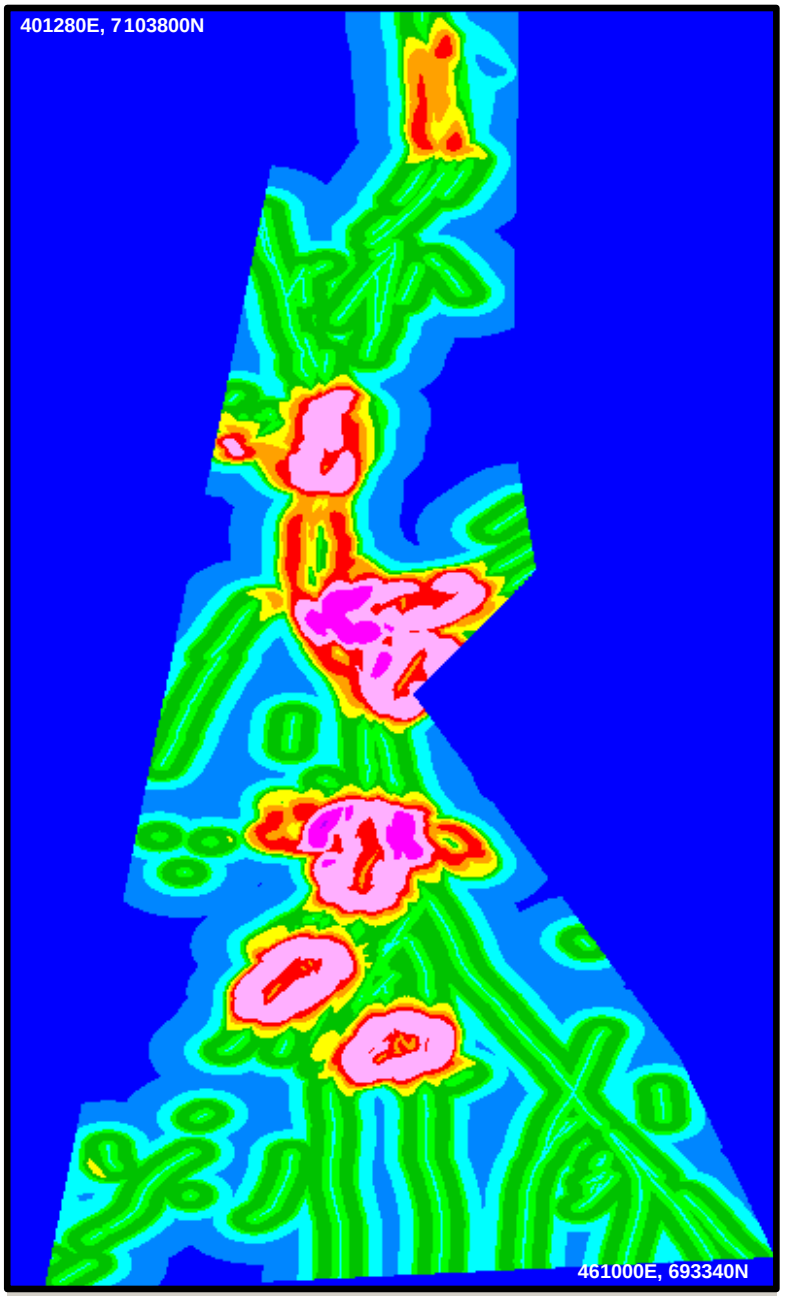

Figure 36: Gold potential map in greenstone belt #16 (no known deposits) (UTM NAD83, Zn12).

supracrustal rocks and permissive faults occur, as shown in Figure 35. Each of the four data layers was generated by computing the shortest distances from the presence of Archean conglomerate, permissive faults, granite-porphyry and ultramafic supracrustal rocks at each pixel

location. The same set of decay functions shown in Figure 12(B) was used to generate the potential map for the greenstone belt in area #16 (Figure 36).

Summary of the results for Slave Province using only three criteria: the location of permissive faults, porphyry-type intrusions and ultramafic rocks

Tables 3, 4 and 5 illustrate the calculated potential content of gold in the various greenstone belts in Slave Province, based on the known amount of gold in the Timmins, Kirkland Lake and Val D'Or districts (see above).

	Study area in km^2	Conglomerate in m^2	Porphyry in m^2	Ultramafic in m^2	permissive faults in m	Potential area in km^2
Timmins-Kirkland	**45,815.00**	**323,250,000**	**1,015,530,000**	**861,330,000**	**3,085,000**	**2,290.00**
Val d'Or	**5,349.00**	**333,230,000**	**18,390,000**	**239,180,000**	**675,400**	**776.00**
xxx	**xxx**	**xxx**	**xxx**	**xxx**	**xxx**	**xxx**
Belt #1: Hope Bay	**8,117.60**	**17,850,000**	**8,142,800**	**1,815,600**	**628,380**	**169.12**
Belts #3 & 4	**24,926.58**	**9,534,800**	**24,877,200**	**0**	**2,230,780**	**20.73**
Belt #5: Hackett River	**12,504.34**	**19,019,600**	**34,454,800**	**0**	**782,960**	**0**
Belt #11	**12,052.08**	**125,208,000**	**48,466,400**	**0**	**1,215,340**	**311.49**
Belt #12	**7,229.04**	**6,845,600**	**10,984,800**	**0**	**1,192,920**	**55.42**
Belt #14: Yellowknife	**4,800.21**	**22,597,200**	**6,120,400**	**0**	**538,800**	**85.96**
Belt #15	**2,436.35**	**2,692,400**	**10,652,400**	**0**	**220,800**	**44.57**
Belt #16	**5,032.50**	**24,405,600**	**192,800**	**10,434,000**	**942,520**	**52.58**

Table 3: Summary of data for the eight Slave Province greenstone belts used to generate prediction maps. The units for "Study area" and "Potential area" are in km^2, the units for "Conglomerate", "Porphyry" and "Ultramafic" are in m^2 and the unit for "permissive faults" is m. For comparison, the same data are shown for the Timmins - Kirkland Lake and Val D'Or areas.

	Potential area in km^2	Discovered gold in Tonnes	Average gold in Tonnes per 1 km^2
Timmins belt	**827**	**2198**	**2.641**
Kirkland belt	**889**	**1326**	**1.491**
Val d'Or belt	**592**	**860**	**1.453**

Table 4: Sizes of potential areas, amounts of gold discovered within two greenstone belts, Timmins and Kirkland shown in Figure 11 and Val d'Or belts shown in Figure 14. The last column was obtained by dividing the amount of gold discovered by the potential area and it shows the average amount of gold in each potential km^2.

	Potential area in km^2	Expected gold in tonnes using Val d'Or belt	Expected gold in tonnes using Timmins belt
Belt #1: Hope Bay	**169.12**	**245.7314**	**446.6459**
Belts #3 & 4	**20.73**	**30.1207**	**54.7479**
Belt #5: Hackett River	**0**	**0**	**0**
Belt #11	**311.49**	**452.5950**	**822.6451**
Belt #12	**55.42**	**80.5253**	**146.3642**
Belt #14: Yellowknife	**85.96**	**124.8999**	**227.0204**
Belt #15	**44.57**	**64.7602**	**117.7094**
Belt #16	**52.58**	**76.3987**	**138.8638**
TOTAL	**739.87**	**1075.0311**	**1953.9967**

Table 5: Size of potential area with two "expected" amounts of gold in each greenstone belt in Slave Province, computed using the potential area in the last column in Table 2 and two average amounts of gold in each potential km^2 in Table 3.

I) Include iron formation as a criterion in two greenstone belts

In addition to the three geological units, Archean conglomerate ("Timiskaming-like" sediments), granite-porphyry and permissive faults, iron formation was added as a key parameter, to generate the following potential map (Figure 37) for greenstone Belts #3 and #4. In comparison with the potential map shown in Figure 24, obtained using only the first three geological units ("Timiskaming-like" sediments), granite-porphyry and permissive faults), the areas of highest potential increase significantly from 20.73 km^2 to 275.10 km^2

Similarly, iron formation was added to the analysis of greenstone belt #5 (Hackett River) to generate the potential map shown in Figure 38. In comparison with the potential map shown in

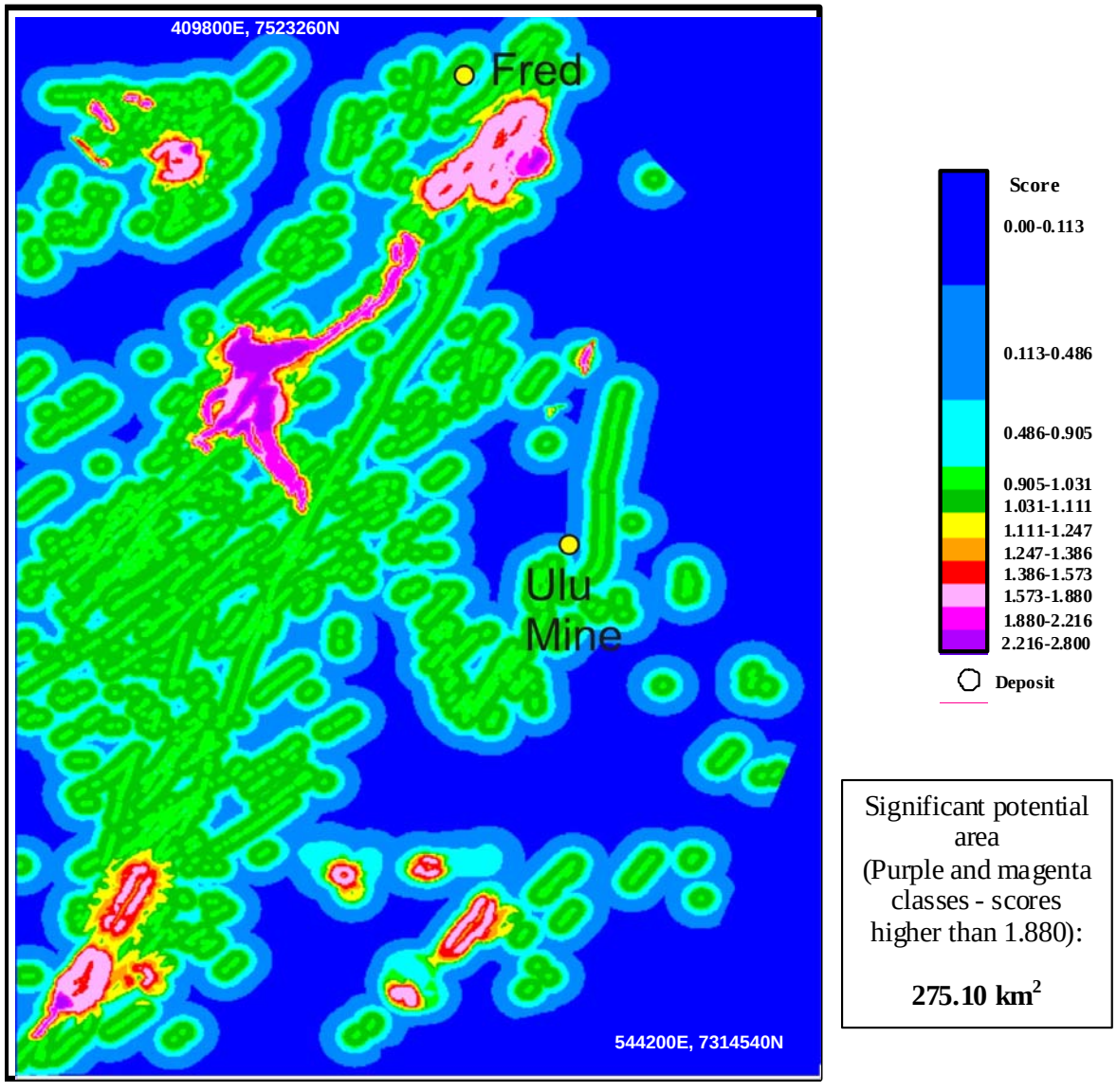

Figure 37: Gold potential map in greenstone belts #3 and 4, using iron formation as an additional criterion (UTM NAD83, Zn12).

Figure 26, obtained using only three geological criteria, in Figure 38 the areas of highest potential increase significantly from 0 km^2 (Figure 26) to 41.40 km^2 (Figure 38).

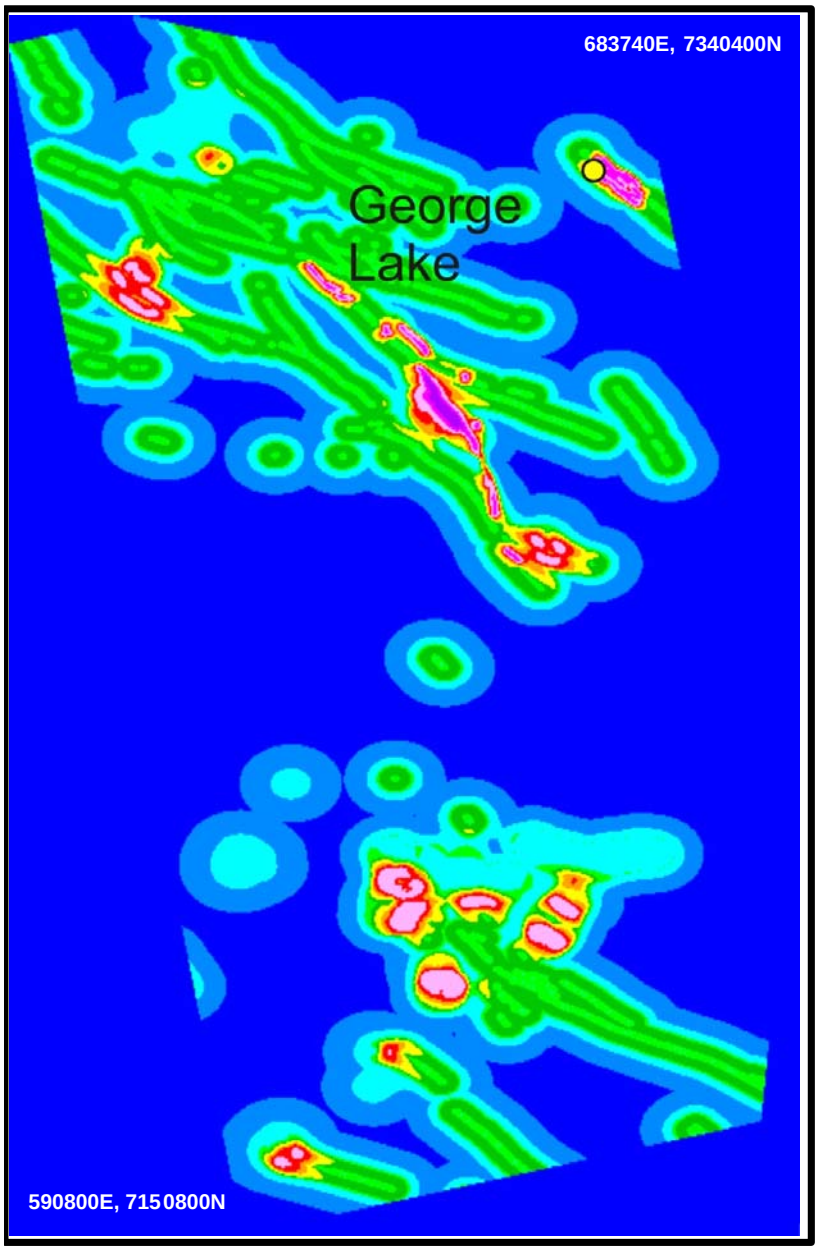

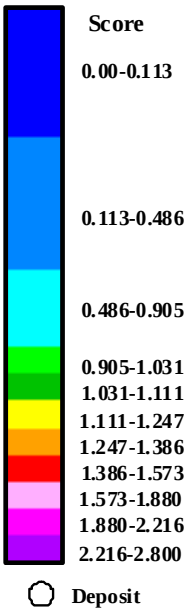

Significant potential area (Purple and magenta classes - scores higher than 1.880):

41.40 km^2

Figure 38: Gold potential map in greenstone belt #5 (Hackett River belt) with the iron formation as an added criterion (UTM NAD83, Zn12).

Effect of adding iron formation:

The changes in gold potential in the two areas where iron formation is recorded in the map are shown in Tables 6 and 7.

	Iron formation in m^2	otential area without on formation in km^2	Potential area with Iron formation in km^2
Belts #3 & 4	**142,494,400**	**20.73**	**275.10**
Belt #5: Hackett River	**6,918,800**	**0**	**41.40**

Table 6: Three greenstone belts #3, #4 (combined into a single map) and #5 (Hackett River) contain iron formation. Two "Potential area" maps are generated, one including iron formation and the other without it.

	Potential area with Iron formation in km^2	Expected gold in tonnes using Val d'Or belt value	Expected gold in tonnes using Timmins belt value
Belts #3 & 4	**275.10**	**399.7203**	**726.5391**
Belt #5: Hackett River	**41.40**	**60.1542**	**109.3374**
TOTAL	**739.87**	**1075.0311**	**835.8765**

Table 7: Size of potential area, two "expected" amounts of gold in two greenstone belts containing iron formation in Slave Province. The predicted amounts of gold in each greenstone belt were computed using the values per unit area (km^2) as determined for Timmins and Val D'Or, and shown in the last column in Table 5.

The gold potential in Belts 3 and 4 increases almost fourteen fold (from 20.73 to 275.1 km^2) for the "most prospective" upper 5% of the areas with assessed potential. Does the small amount of abundant porphyritic intrusions or Temiskaming-type conglomerate indicate that these belts have relatively poor potential, and that the presence of iron formation might skew our analysis? Perhaps not, given the lack of detailed mapping in these greenstone belts.

J) Summary of Slave Province Evaluation

The evaluation of Slave Province for its gold potential indicated that many areas with few or no known gold occurrences have good potential for discovery, as illustrated in Figure 39, but several issues are worth noting:

1: The applicability of this method for assessing the potential for the occurrence of economic gold deposits worked only moderately well. We determined the greenstone belt areas purposely without knowledge of the locations of the gold deposits, in order to make our study clearly a "blind test" of the method. The presence of Archean volcanic rocks was the only criterion that we used in establishing the greenstone belt polygons. Eight of the 33 deposits or occurrences in Slave Province that contain sufficient resources to be included in various databases are not in these polygon areas. Most of these are within 10 km of the polygons used to define the individual greenstone belts, and are vein systems contained in metasedimentary strata. This includes the Lupin Mine, a significant gold producer. A few are in isolated, poorly mapped areas such as the Goose Lake and Boot Lake occurrences The geological data for the greenstone belt that contains the Tundra Mine, another significant past-producer, did not allow for evaluation .

Only 9 out of 16 greenstone belts could be assessed. These contain 21 of the 33 deposits and occurrences, or 21 of 25 occurrences that are in the selected greenstone polygons. The remaining belts were lacking any indication of the presence of a sufficient number of key criteria to enable its use. Adding iron formation into the list of key criteria definitely improves the estimation of potential for those polygons lacking other criteria. However, the variability of the quality of the information in this map rendered its use somewhat uncertain. For example, the Lupin Mine, a significant gold producer, does not, on the map, appear to have associated iron formation, yet the deposit occurs within this rock type. The lack of presence of Temiskaming-type conglomerate in the un-assessed seven belts may be a true reflection of the absence of this rock type, or inaccurate classification of it. The latter may be more accurate. Bleeker and Hall (2007) provide a more detailed map of the George Lake area, for example, where they note coarse clastic (Temiskaming-like) strata, late felsic porphyry intrusions, iron formation and major fault-shear zones. Should these have been contained in the Stubley (2005) compilation, our assessment of this area would have been successful There is less likelihood that ultramafic rocks could have been mis-mapped, however, and these seem to be much less abundant in many of the greenstone belts in Slave Province.

In summary, better definition of what constitutes a "greenstone belt", and more extensive and consistent representation of the key attributes, would have enhanced our ability to assess all of Slave province. Given that the Stubley (2005) compilation is the first comprehensive compilation map, and that 21 out of 25 deposits were in the tested areas, the resulting assessment is considered moderately successful. Our model requires some adjustment, to include areas that contain at least three of the key criteria, but that need not contain volcanic strata as one of these.

2: Only the Yellowknife greenstone belt has “mature” gold production, and the mapping base there is on a par with that for the Timmins, Kirkland Lake and Val d’Or districts. The method was reasonably successful for Yellowknife, with the two largest deposits, Con and Giant, along with the nearby Crestaurum and Mon deposits occurring in the area with the uppermost 5% potential. These represent almost 90% of the gold mined or in resources in the camp. The third deposit, the Discovery Mine, is just outside the area of highest potential. All of the other occurrences are in the upper 50% of the rated regions. The model significantly underestimates the amount of gold to be discovered in the Yellowknife area: using the Val D’Or model, there is potential for discovery of 124.9 tonnes (227 tonnes using the Timmins model) , but data from NRCan compilation tables indicate that past production or resources total 541 tonnes of gold.

3: The method worked successfully in the Hope Bay district, and identified all three of the known deposits within the upper 10% of the prospective areas, and two of these are within the upper 5%. Using the more conservative Val D’Or model, the analysis indicates that about 245 tonnes of gold might be discovered in the district and 447 tonnes by the Timmins model. It presently contains at least 111 tonnes, and is still being actively explored.

4: The other areas for which we were able to provide resource estimates all contain developed prospects, and a few mines. All of the deposits and occurrences fall within the upper 50% of the estimated areas, with many in the upper 10-15%. Notably, the mines in areas 3 and 4 corresponded rather poorly to our predicted zones of highest potential. The accuracy of predicting the known deposits is not as good as it was for the Timmins, Kirkland Lake or Val d’Or areas. Although we successfully predicted the presence of at least 75% of the gold contained in resources, this prediction could have been much better if the regional geological database had been more accurate, and our model requires adjustment to include sedimentary-dominated terrains as well as those that are volcanic-dominant.

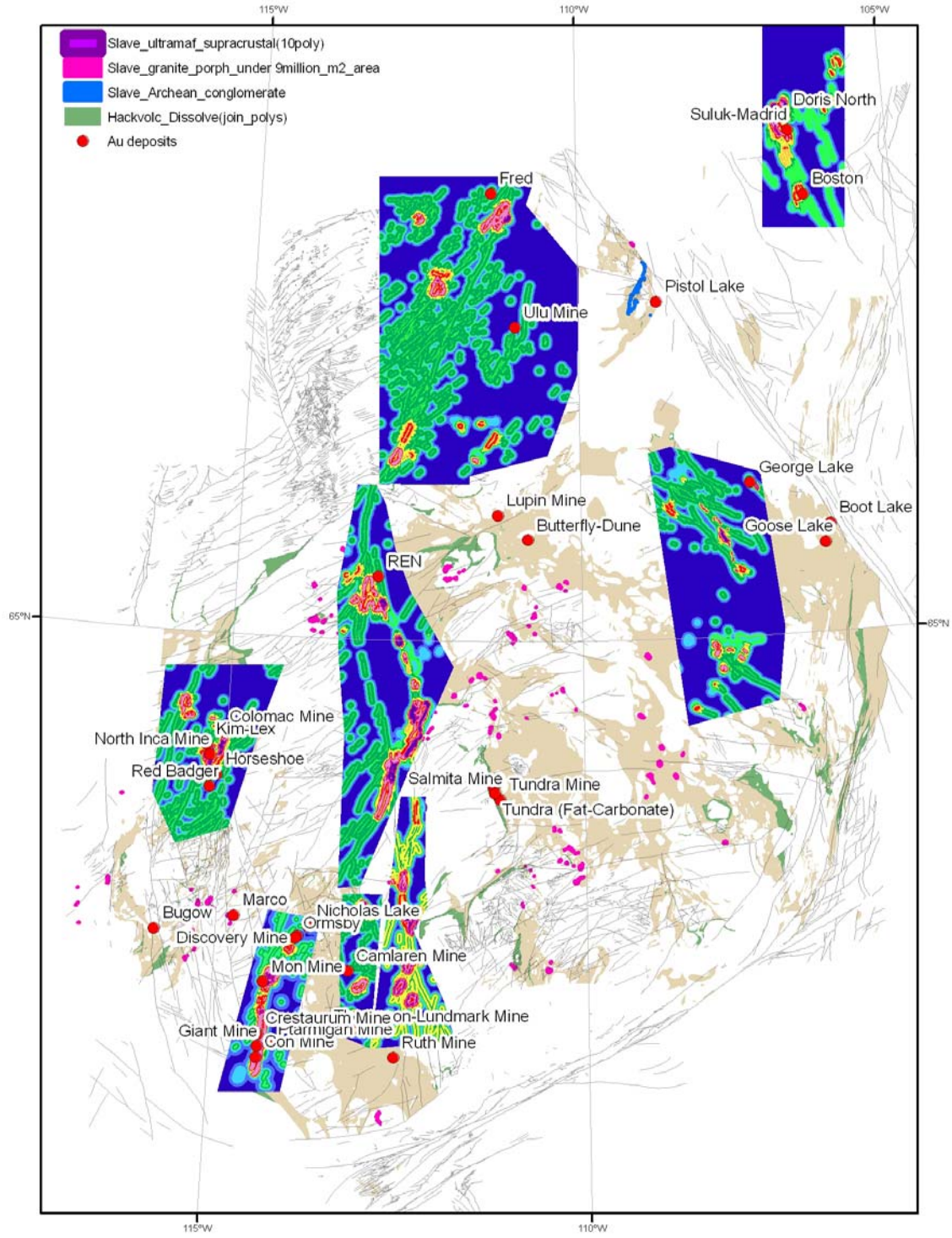

Figure 39: Major gold deposits in the Slave Province and compilation of gold resource potential maps.

Summary and Recommendations

a) Method Development

1: We used a limited set of key criteria, based on observations of all of Canada's orogenic gold deposits, to assess the potential for discovery of gold resources. These are:

1. All are within broadly defined "greenstone belts". These typically have a significant component of volcanic strata, but may contain abundant sedimentary strata as well.
2. Presence of major fault/shear zones, typically 10's to 100's of km in overall length
3. Presence of unconformities, delineated by extensional basins filled with late- tectonic, post-arc coarse clastic rocks, typically "Temiskaming-like" fluviatile conglomerate, arkose or sandstone.
4. Presence of small (200m-2km in diameter) felsic or alkaline intrusions.
5. Presence of highly ductile ultramafic rocks adjacent to less ductile tholeiitic volcanic or other easily fractured supracrustal strata
6. Presence of iron formation or similar reactive rock type

2: We selected the Timmins-Kirkland Lake area as our primary test site, and Val D'Or as a second "proof of concept" test area. Both areas have recent high-quality digital compilation maps, and world-class gold deposits. In preparing the maps for analysis, we purposely ignored the presence of the gold deposits.

3: The most significant task in preparing the maps was to analyze the fault groupings by strike. To do this, we established the prominent strike of the supracrustal rocks by dividing their contacts into short (100 to 200m) lengths, and determined the tangents to the strike of the midpoints of these segments. Area for analysis should be chosen on the basis that they have a single prominent strike direction. In both our test areas, this is close to 90^{o}. Using a histogram analysis we determined the prominent strike direction, and selected the central 50% of that distribution to represent the regional strike. Then, using a similar methodology, we determined the most prominent strike directions of the faults in the map area. These typically are in at least two, and commonly three distinct azimuthal packages. We then chose only those faults with the same strike range as that representing the regional supracrustal strata. In the Timmins test, the major faults are related to the Destor Porcupine regional fault/shear system, a 300+km-long major transpressive zone. In the Val D'Or and Kirkland Lake areas, this is the 350km-long Cadillac-Malartic "break". In both cases, our method for selecting the most prospective fault systems worked well.

4: Selecting the appropriate late-tectonic coarse clastic rocks was relatively simple in the two test areas, as these have long been clearly identified on maps as late-tectonic clastic strata. Selecting the appropriate intrusions was a bit more challenging, so we limited the size of these to about 50 km^2. In both the Ontario and Quebec systems these are identified as "late" Archean intrusions, and because of the robust geochronological database that underpins these maps, the identification of these was relatively reliable.

5: Selection of the ultramafic rocks and iron formations was quite straightforward; we allowed some latitude in what was included in the ultramafic group, to allow both volcanic and stratiform intrusive ultramafic bodies. We gave a stronger weighting to komatiitic flows and strictly ultramafic intrusions, and a lower rating to those classified as "mafic-ultramafic".

6: All of the geological data were then coded into pixels, each typically $50m^2$.

7: We developed a set of curves to mathematically reduce the value of an observation as a function of the distance away from the observation. These 'decay curves', one for each of the key criteria listed above except the presence of volcanic rocks, have a set of parameters that include their reliability or importance to the model (e.g. a high value of 0.8 to 1 for the faults, but less for the others, including a value of only 0.3 for the ultramafic rocks), the distance from the observation point for each criterion that is ideal for gold deposit occurrence, and a maximum distance away from the observation point beyond which the value of that criterion is set to 0. All of these decay curves take the form of a skewed log-normal distribution curve, with "peak distances (those most favourable for gold occurrence as a distance away from the observation point) of from 1000 to 2500meters, depending on the criterion.

8: The analysis was then performed by starting at the pixel at the uppermost corner of the map area, and measuring the shortest distance to each criterion (2 to 5 above for our Ontario and Quebec tests, and 2-6 for Slave Province) from it, then decaying the value of the criterion as a function of the distance away from it, using the appropriate decay curve. A score value for each pixel was then established by adding the values determined for each criterion. These were then converted into percentage ranks by dividing the range of scores by the number of pixels. The largest score being a higher probability of a gold occurrence, the lowest has no probability of occurrence. Once all pixels were analyzed, the scores or ranks were contoured, producing a map of gold potential.

b) Results

The contoured maps rather remarkably outlined the areas of most abundant gold deposits. In order to determine the efficacy of the method, we analyzed the value of gold contained as deposits within the various contour intervals.

1: The uppermost approximately 5% percent of the contoured area occupying 2,291km^2 contains 96.3% (3,524 tonnes) of the gold contained in production or resources. For Timmins, 2,198 tonnes of gold are within 827km^2, and for Kirkland Lake 1,326 tonnes of gold are within 889 km^2. In the Val D'Or district, 93.2% (860 tonnes) of the gold occurs in the upper 5% of the contoured area, or about 592km^2. Thus, the uppermost 5% of the contoured area contains 2.641 tonnes per km^2 at Timmins, and 1.49 tonnes/km^2 and 1,463 tonnes per km^2 in Kirkland Lake and Val D'Or respectively.

Overall, the resource assessment method established herein "discovered" the know resources exceptionally well. On each map, there are significant areas of high potential that contain only small deposits and occurrences. Either we have over-estimated the size of the areas of best potential or these areas deserve further prospecting. Regardless, the method provides a first-order guide to the most prospective areas, and the results reduce risk for exploration.

2: For Slave Province, the application of the method had some shortcomings. Although it successfully "re-discovered" much of the gold either produced or in resources in the various greenstone belts, it was less successful at this. Only about 75% of the deposits with reserves were in the upper 10% of the contours. Only about 2/3 of the greenstone belts could be analyzed. The reasons for the poorer success at applying the method to the Slave areas include:

a) Many of the gold deposits in Slave occur in sediment-dominated areas, but we used the distribution of volcanic rocks as the primary way to select areas for analysis. Our model needs to be broadened to accommodate these sedimentary-dominated areas. Rather than predetermining the areas to be studied on the basis of the presence of volcanic strata only, we should have determined the distribution of all 6 criteria listed above, and then established sub-regions strictly on the basis of their structural trend.
b) The compilation map was designed for display at a scale of 1:1 million. By comparison, the maps for Ontario and Quebec were compiled for display at a scale of 1:100,000. Furthermore, the latter map databases were compiled from very robust, consistent, modern, and typically 1:50,000 maps. These were updated by additional field work. Slave geology was compiled from a variety of sources, some only reconnaissance in scale. Only the Yellowknife area has a recent and consistent geological map base underpinning it.
c) The use of iron formation as a key consistent improved the analysis considerably. Iron formation should be included in all such assessments. This would have made little difference to the quality of the Ontario and Quebec assessments, but many other gold-rich districts, such as Geraldton, Pickle Lake and Musselwhite in Ontario have iron formation as a major, ore-related constituent.
d) Much more consistent and useable legends need to be developed for GSC maps. The current legend scheme attempts to encompass age, formational name, lithotype and alteration into a single legend identifier, making deconvolution of the map into polygons for which we can establish the presence of the six criteria listed above quite challenging.

e) Map compilation is an on-going process, but clearly there are many domains within the north that require re-mapping. The level of detail required for exploration, and ideally to underpin the type of analysis undertaken herein, requires high-quality 50:000-scale mapping. As a start, each of the areas for which we could not undertake an analysis, because of possible poor data quality, should be considered for re-mapping.

3: In spite of these short-comings, our analysis indicates that Slave Province contains a total of between 1504 (Val D'Or model) and 2736 (Timmins model) tonnes of gold, and as yet, only about 961 tonnes exist in mined reserves or resources. Such potential contents are, of course highly speculative, but based on the comparison between our estimates and the contents in established camps in Slave, they are possibly conservative. Much gold remains to be discovered in Slave!

c) Recommendations

1. That the Stubley (2005) compilation be upgraded, and the analysis repeated.
2. The maps for Rae and Hearne provinces are in progress: these should also be analyzed, using all of the above criteria.
3. The criteria should be refined to encompass sedimentary – dominated areas
4. That methodology should be established to deal with folded major fault systems, such as exist in the Rae and Hearne provinces, where Proterozoic deformation has been superimposed on Archean structures as well as its stratigraphic elements.
5. The method should be applied to well-mapped areas, such as Geraldton, Meadowbank or Musselwhite, where gold is contained at least in part in iron formation. Based on this improvement, the criteria may be refined to adapt better to sedimentary-dominated areas.
6. For areas in Slave province where the predicted areas of highest potential correspond poorly with the location of the known occurrences (e.g. areas #3 and #4), detailed maps of the areas be examined (or obtained with new mapping) to investigate whether the model or the geological database (as per the George and Goose Lake areas) is the cause of this poor fit.

References

Ayer, J. A., Trowell, N. F., and Josey, S., 2004, Geological compilation of the Abitibi greenstone belt: Ontario Geological Survey, Miscellaneous Release–Data 143.

Bleeker, W., and Hall, B., 2007, The Slave Craton: Geology and metallogenic evolution, *in* Goodfellow, W. D., ed., Mineral Deposits of Canada: A Synthesis of Major Deposit-Types, District Metallogeny, the Evolution of Geological Provinces, and Exploration Methods: Geological Association of Canada, Mineral Deposits Division, Special Publication No. 5, p. 849-879.

Brisbin, D.I., 1997, Geological Setting of Gold Deposits in the Porcupine Gold Camp, Timmins, Ontario: Ph.D. thesis, Queen's University, Kingston, Ontario, 523 p.

Chung, C.F., Franklin, J.M. and Hillary, E.M., 2011, Development of a GIS-based System for Assessment of Discovery Potential Using an Expert-Defined VMS Deposit Model and Digital Geological Maps: Geological Survey of Canada, Open File 6764, 67 p.

Dubé, B., Balmer, W., Sanborn-Barrie, M., Skulski, T., and Parker, J. 2000, A preliminary report on amphibolite-facies, disseminated-replacement-style mineralization at the Madsen gold mine, Red Lake, Ontario: Geological Survey of Canada, Current Research 2000-C17, 12p.

Dubé, B., and Gosselin, P., 2007, Greenstone-hosted quartz-carbonate vein deposits, *in* Goodfellow, W.D., ed., Mineral Deposits of Canada: A Synthesis of Major Deposit-Types, District Metallogeny, the Evolution of Geological Provinces, and Exploration Methods: Geological Association of Canada, Mineral Deposits Division, Special Publication No. 5, p. 49-73.

Dubé, B., Williamson, K., and Malo, M., 2003, Gold mineralization within the Red Lake Mine trend: example from the Cochenour-Willans Mine area, Red Lake Ontario with some new key information from the Red Lake Mine and potential analogy with the Timmins camp: Geological Survey of Canada, Current Research 2003-C21, 15 p.

Dubé, B., Williamson, K., McNicoll, V., Malo, M., Skulski, T., Twomey, T., and Sanborn-Barrie, M., 2004, Timing of gold mineralization in the Red Lake gold camp, northwestern Ontario, Canada: new constraints from U-Pb geochronology at the Goldcorp High-grade Zone, Red Lake mine and at the Madsen mine: Economic Geology, v. 99, no. 8, p. 1611-1641.

Goldfarb, R. J., Baker, T., Dubé, B., Groves, D. I., and Gosselin, P., 2005, Distribution, character and genesis of gold deposits in metamorphic terranes, *in* Hedenquist, J. W., Thompson, J. F. H., Goldfarb, R. J., and Richards, J., eds., One Hundredth Anniversary Volume: Society of Economic Geologists, p. 407-450.

Hodgson, C.J., 1993, Mesothermal lode-gold deposits, *in* Kirkham, R.V., Sinclair, W.D., Thorpe, R.I., and Duke, J.M., eds., Mineral Deposits Modelling: Geological Association of Canada, Special Paper 40, p. 635-678.

Hodgson, C.J., and MacGeehan, P.J., 1982, Geological characteristics of gold deposits in the Superior Province of the Canadian Shield, *in* Hodder, R.W., and Petruk, W., eds., Geology of Canadian Gold Deposits: Canadian Institute of Mining and Metallurgy, Special Volume 24, p. 211-229.

Houlé, M. G., Ayer, J. A., Baldwin, G., Berger, B. R., Dinel, E., Fowler, A. D., Moulton, B., Saumur, B.-M., and Thurston, P. C., 2008, Stratigraphy and Volcanology of Supracrustal Assemblages Hosting Base Metal and Gold Mineralization in the Abitibi Greenstone Belt, Timmins Ontario: Geological Association of Canada - Mineralogical Association of Canada, Field Trip Guidebook, 84 p.

Ispolatov, V., Lafrance, B., Dubé, B., Creaser, R., and Hamilton, M., 2008, Geological and structural setting of gold mineralization in the Kirkland Lake-Larder Lake gold belt, Ontario: Economic Geology, v. 103, No. 8, p. 1309-1340.

Kerrich, R., Goldfarb, R., Groves, D., and Garwin, S., 2000, The geodynamic of world-class gold deposits: characteristics, space-time distribution and origins: SEG Reviews, v. 13, p. 501-551.

Lamothe, D., Harris, J. R., Labbé, J.-Y., Doucet, P., Houlé, P. J. M., Dion, C. R. S., and Moorhead., J., 2005, Évaluation du potentiel en minéralisations de type sulfures massifs volcanogènes (SMV) pour l'Abitibi, EP 2005-01, 1 CD-ROM., Ministère des Ressources naturelles, de la Faune et des Parcs, Quebec City.

Poulsen, K.H., Card, K.D., and Franklin, J.M., 1992, Archean tectonic and metallogenic evolution of the Superior Province of the Canadian Shield: Precambrian Research, v. 58, p. 25-54.

Poulsen, K. H., Robert, F., and Dubé, B., 2000, Geological classification of Canadian gold deposits: Ottawa, Geological Survey of Canada Bulletin 540,106 p.

Robert, F., 1990, Structural setting and control of gold-quartz veins of the Val d'Or area, southeastern Abitibi subprovince, *in* Gold and base-metal mineralization in the Abitibi subprovince, Canada, with emphasis on the Quebec segment: Geology Department (Key Centre) & University Extension, The University of Western Australia; Publication No. 24. p. 167-210.

Robert, F., 2001, Syenite-associated disseminated gold deposits in the Abitibi-greenstone belt, Canada: Mineralium Deposita, v. 36, p. 503-516.

Robert, F., Poulsen, K. H., Cassidy, K. F., and Hodson, C. J., 2005, Gold metallogeny of the Superior and Yilgarn cratons, *in* Hedenquist, J. W., Thompson, J. F. H., Goldfarb, R. J., and Richards, J., eds., One Hundredth Anniversary Volume, Society of Economic Geologists, p. 1001-1033.

Stubley, M. P., 2005, Slave Craton: Interpretive bedrock compilation, Digital files and 2 maps: Yellowknife, Northwest Territories Geoscience Office, Open File 2005-01.